$\mathcal{I}\,\omega$

PB88-207782

Commission of the European Communities

physical science

MONITORING OF CARBURISATION
BY THE USE OF MAGNETIC TECHNIQUES,
PART I, FUNDAMENTAL ASPECTS
AND MEASUREMENTS ON 25 Cr20Ni STEELS

E. LANG, J.F. NORTON
Commission of the European Communities
Joint Research Centre
Petten Establishment
PETTEN (The Netherlands)

1986

EUR 10566 EN

1L

LEGAL NOTICE

Neither the Commission of the European Communities nor any person acting on behalf of the Commission is responsible for the use which might be made of the following information

50272-101

I

REPORT DOCUMENTATION PAGE	1. REPORT NO. EUR 10566	2.	3. Recipient's Accession No.

4. Title and Su Monitoring of carburisation by the use of magnetic techniques, Part 1: fundamental aspects and measurements on 25 Cr20Ni steels		5. Report Date 1986
		6.

7. Author(s) LANG E, NORTON J F	8. Performing Organization Rept. No.

9. Performing Organization Name and Address	10. Project/Task/Work Unit No.
	11. Contract(C) or Grant(G) No. (C) (G)

12. Sponsoring Organization Name and Address	13. Type of Report & Period Covered
	14.

15. Supplementary Notes

CUSTOMERS IN THE EUROPEAN COMMUNITY COUNTRIES SHOULD APPLY TO THE OFFICE FOR OFFICIAL PUBLICATIONS OF THE EUROPEAN COMMUNITIES, B. P. 2985, LUXEMBOURG.

16. Abstract (Limit: 200 words)

The use of non-destructive, magnetic analysis as a means of monitoring the corrosion of alloys has been suggested by several researchers. The present study reports on the effect of carburisation on the magnetic properties of some austenitic steels.

The change of magnetic properties has been measured at room temperature using a magnetic-balance (set-up following Rankine). Alterations in the Curie-point of the alloys have been monitored by thermomagnetometry.

The possibility of relating the development of ferromagnetic properties to the extent of carburisation is discussed and the problems involved in making such correlation are considered in detail. It is shown that a number of physicochemical and metallurgical factors are involved and these play an important role in the relationship between magnetic properties and carburisation.

It is concluded that although considerable magnetic changes result from the ingress of carbon and the formation of carbides, a number of factors complicate the use of such changes to quantitatively monitor the progress of carburisation.

17. Document Analysis a. Descriptors

b. Identifiers/Open-Ended Terms

Foreign Technology

c. COSATI Field/Group

18. Availability Statement UNLIMITED DISTRIBUTION	19. Security Class (This Report) UNCLASSIFIED	21. No. of Pages 68
	20. Security Class (This Page) UNCLASSIFIED	22. Price E04 14.50

(See ANSI-Z39.18)   See Instructions on Reverse

OPTIONAL FORM 272 (4-77)
(Formerly NTIS-35)
Department of Commerce

Contents

Abstract

1. Introduction   1

2. Carburisation and change in magnetic properties   2

3. Experimental details   8
    3.1. Methods of magnetic measurements   8
    3.2. Test materials and carburising conditions   10

4. Presentation of results   12
    4.1. As-received condition   12
    4.2. Carburised specimens   13
    4.3. Kinetic studies   16
    4.4. Variation of magnetic response with depth of
          carburisation   19
    4.5. Thermomagnetic analysis of a carburised alloy   22

5. Discussion   23

6. Conclusions   26

    References   29

    Figures & Captions   31

    Appendix I : Effect of various experimental parameters on
                 magnetic response measurements   56

Abstract

The use of non-destructive, magnetic analysis as a means of monitoring the corrosion of alloys has been suggested by several researchers. The present study reports on the effect of carburisation on the magnetic properties of some austenitic steels.

The change of magnetic properties has been measured at room temperature using a magnetic-balance (set-up following Rankine). Alterations in the Curie-point of the alloys have been monitored by thermomagnetometry.

The possibility of relating the development of ferromagnetic properties to the extent of carburisation is discussed and the problems involved in making such correlations are considered in detail. It is shown that a number of physicochemical and metallurgical factors are involved and these play an important role in the relationship between magnetic properties and carburisation.

It is concluded that although considerable magnetic changes result from the ingress of carbon and the formation of carbides, a number of factors complicate the use of such changes to quantitatively monitor the progress of carburisation.

1. Introduction

Industrial experience has shown that the radiant coils of cracking furnaces for ethylene production (pyrolysis tubes) carburise during operation and that this carburisation becomes more important as operating time and temperature increase. Internal carbide precipitation resulting from the reaction of alloying elements with the high carbon activity environment at operating temperatures of 900-1050°C leads to considerable volume increases and changes in thermal conductivity and expansion coefficient of the carburised zone. This in turn may promote higher stresses in the tube section, particularly during thermal transient conditions such as running up/shutting-down procedures thereby shortening the service life of such furnace tubes. There is therefore a strong interest in the non-destructive monitoring of the degradation by carburisation of such tubes in order to ensure their substitution well in advance of an onstream failure which could imply potentially severe economic losses coupled with the possibility of additional damage to the plant.

Several techniques are available which have been used with varying success for regular furnace tube inspection among which magnetic permeability measurements have gained some importance for monitoring the extent of carburisation in radiant coils (1-6).

The apparent advantages of magnetic measurements for the assessment of corrosion attack are evident in that the technique does allow non-destructive testing in a simple and relatively cheap way (e.g. instrumentation) including also the possibility for automatic scanning of large industrial components. It is reported (4) that eventually creep damage, when associated with fissures reaching the (tube) surface and being strongly oxidised, can also be monitored by this techniques.
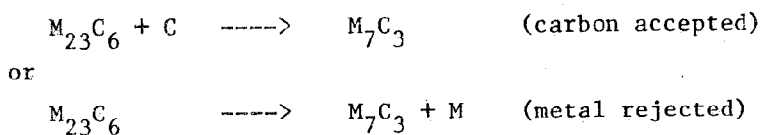
However, considerable controversy has arisen regarding the significance of magnetic readings to indicate remaining tube life (4,5,6). The major problem appears to originate from the fact that the absolute readings of magnetic permeability depend, amongst other features, upon the alloy composition and structure - which can change during service - and hence are not unambiguously related to the amount of carbon picked up or depth

of carburisation. It was therefore concluded that magnetic measurements
could only reasonably be applied to follow the relative progress of
corrosive attack on individual tubes which requires that failure criteria
must be established on basis of standard test results (6). It was pointed
out by several workers (1,4,5,6) that the whole matter is rather complex
and requires a more fundamental study of the magnetic properties of
carburised high temperature alloys before reliable application for
life-time predictions in industrial plants can be made.

Within the frame of the JRC Petten corrosion/ carburisation project
attempts have therefore been made to examine in greater detail some of the
factors involved in the use of magnetic measurements for monitoring the
extent of carburisation. The following report presents the first results
and preliminary conclusions of investigations carried out primarily on the
25Cr-20Ni class of stainless steel.

2. Carburisation and change in magnetic properties

During the carburisation process carbon is picked up by the material
exposed to the corrosive environment and subsequently diffuses into the
matrix, i.e. is adsorbed/absorbed. When the local carbon concentration
exceeds the solubility limit, which is a function of the alloy composition
and temperature, precipitation of carbides of the type $M_{23}C_6$ will occur.
With further supply of carbon this carbide will transform to M_7C_3
according to the reactions,

$$M_{23}C_6 + C \quad \longrightarrow \quad M_7C_3 \qquad \text{(carbon accepted)}$$

or

$$M_{23}C_6 \quad \longrightarrow \quad M_7C_3 + M \quad \text{(metal rejected)}$$

where for austenitic steels M is dominantly Cr (7,8,910). With continuing
time, the carbide transformation front will penetrate into the material
until equilibrium is established between the carbon activity in the alloy
and in the surrounding atmosphere.

Since the migration of carbon in the alloy matrix and the carbide
precipitation are diffusion controlled processes, a carbon concentration

profile will develop, the shape of which (see fig. 1) is dependent upon temperature, time, alloy composition and carbon activity of the environment, and which can be described by modified Fick's laws which take account of precipitation (9,10).

It is generally agreed that the higher the surface carbon content and the steeper the concentration gradient, the more detrimental is the effect of carburisation on the mechanical properties - especially under thermal and/or load cycling conditions (1).

The extent of carburisation is somewhat difficult to define since it depends on the way of detection as indicated in fig.2. In some studies the location of the $M_7C_3/M_{23}C_6$- transformation front is taken as a measure of carburisation, while other workers refer to the depth at which the original carbon content of the alloy is reached.

The precipitation of carbides involves an alteration of the chemical composition of the affected matrix zone. Since the carbides formed are generally richer in Cr than the original austenitic alloy (8,10), their formation implies a depletion in Cr of the carburised matrix zone, i.e. with proceeding carbide precipitation, the composition of the affected matrix zone in a FeCrNi-alloy will move towards the binary Fe-Ni-system as indicated in fig. 3 for different possible carbide compositions (8).

Bühler et al. (8) have further pointed out that for relatively lean austenitic steels, e.g. X 15 CrNiSi 20 12, Cr-depletion due to carbide precipitation may raise the $\gamma \longrightarrow \alpha'$-tranformation temperature above room temperature, hence martensite may form within the carburised zone on cooling such a steel after carburisation to ambient temperature.

These changes in composition and/or structure may be accompanied by corresponding alterations of the mechanical and physical properties, and if these include the magnetic state of the affected alloy zone, i.e. a change from paramagnetic to ferromagnetic behaviour, then the progress of carburisation can potentially be monitored by measurements of magnetic permeability.

At this point it is perhaps pertinent to review some of the principles
of solide state magnesium : Most metals are para- or diamagnetic, and only
Fe, Ni, Co and some rare earth elements show ferromagnetic behaviour.
Ferromagnetic materials have a very high positive susceptibility which
depends in a complex way on temperature and magnetic field. These
substances become paramagnetic above a certain critical temperature T_c
(Curie-point).

The theory of magnetism (11) describes how ferromagnetic metals by
alloying with each other or with non-ferromagnetic elements (e.g. Cr, Ti,
Al..) may become para- or even diamagnetic. The ferromagnetism of e.g.
nickel is known to originate from the fact that the partially filled $3d^+$
and $3d^-$ electron shells are occupied by an unequal number of electrons
with opposed electron spin, i.e. magnetic moment : 5 and 4,4 electrons
respectively. This occupancy difference results in an overall magnetic
moment of the metal. By alloying Ni with Cr for example, the "holes" in
the 3d-electron shells become filled with the Cr-valency electrons whereby
the resulting magnetic moment becomes zero. Above a certain critical
Cr-concentration the alloy will be non-ferromagnetic. This is - in a
simplified way - the reason why most high-temperature alloys which lie in
the austenitic region of the Ni-Cr-Fe system are paramagnetic with
permeabilities in the range 1,00-1,05 - at least at temperatures $T \geq RT$.
However, it must be pointed out that due to the temperature dependence of
the electron shell occupancy, austenitic alloys may also become
ferromagnetic at lower temperature ($T \leq RT$) since the Curie-Temperature is
a complex function of the composition of Fe-Ni-Cr-alloys. This has been
studied in some detail by several workers (12, 13, 14). In addition, the
permeability (susceptibility)*[)] of ferromagnetic alloys is also related to
alloy composition since the resulting magnetic moment depends on the
electron state of the alloy.

Since ferromagnetism is a solid state phenomenon, the (lattice)
structure of the material under consideration will determine its magnetic
state. A typical example is 18/8 CrNi stainless-steel which is
paramagnetic at room-temperature. However, when cooled in liquid nitrogen
the α (bbc)-structure is induced by the martensitic transformation and

---

*[)] The relation between permeability μ and susceptibility X is given by :
$\mu = 1 + 4 \pi X$.

having a Curie-temperature of ca. 400°C this phase is ferromagnetic at room-temperature.

To summarise, it may be stated that ferromagnetic materials can be identified by their (high) permeability value (μ), which depends upon magnetic field strength, and their specific Curie-temperature (T_c), both of these being dependent on composition and structure of the alloy. In particular for austenitic Fe-Ni-Cr-steels, T_c and μ vary strongly with the Cr/Fe+Ni ratio.

From the preceding discussion it is obvious that when a process (e.g. carbide precipitation) is to be monitored by measurements of magnetic properties, the measurements must be taken at $T_m < T_c$ [*] because for $T_m > T_c$ the structural development or compositional alteration might only be reflected by changes of the paramagnetic susceptibility values. In general these would be difficult to measure, since they are small and depend in a much less pronounced way on alloy composition.

As a result of the precipitations of Cr-rich carbides due to carbon uptake; the composition of the residual alloy matrix varies in a continuous fashion throughout the carburised zone, a typical example for this being shown in Fig. 4 indicating in particular the severe Cr-depletion mentioned before. This zone of varying composition can be represented in a schematic way by a series of thin layers (n) of equal thickness (volume) and of different homogeneous composition (Fig. 5). It has already been stated that the Curie-temperature of Fe-Ni-Cr-alloys increases rapidly with decreasing Cr-content (12, 13, 15); in addition, the permeability may also vary with the Cr-concentration (14). Hence each of the layers will have a specific Curie-temperature and also a different permeability value according to its composition. The overall temperature dependence of the magnetic permeability of the depleted zone can therefore be represented by the sum of the curves for the individual layers as shown in fig. 5 a+b. In fig. 5a it is assumed that the compositional change is only affecting the Curie-temperature of the alloy layers, and in fig. 5b

---

[*] T_m = temperature of measurement
T_c = Curie-temperature.

the assumption is made that both T_c and permeability μ are being altered as a consequence of the compositional gradient. It is also obvious from this schematic figure that the measured overall change in permeability due to the presence of a carburised zone will depend on the relative location of the measurement temperature with respect to T_c (min) and T_c (max). This is also essential when referring to fig. 2 since it means that the extent of carburisation monitored by magnetic measurements will depend on the temperature of measurement, i.e. it will increase with decreasing temperature since with decreasing temperature the deeper, Cr-richer layers (see fig. 5) may also become ferromagnetic.

Summarising, it can be stated that magnetic measurements will reflect changes in the matrix element composition and distribution caused by the carbide precipitation*[)], and that as long as carburisation continues, from the associated element partitioning of the austenite, i.e. the changing ratio between ferro- and paramagnetic elements, a change of the permeability, when measured at $T_m < T_c$, is to be expected. A further implication from the above model is that T_c (surface) will remain constant (= T_c max) and T_c (bulk) will increase. In addition, it is obvious that the change from para- to ferromagnetic state of a certain volume of material (dV) will be easily detected because of the large difference in suscpetibility ($1:10^5$), while a change of the ferromagnetic permeability value may give rise to less drastic variations. This point appears important because the onset of carburisation may transform the outer layer of the paramagnetic alloy by precipitation of $M_{23}C_6$-carbides into a ferromagnetic austenite (fig. 6). During further carburisation, this carbide layer will be transformed into M_7C_3. This transformation would not involve any further change in permeability if the metal partioning in both carbides was the same. It is known (7, 8, 10) however, that $M_{23}C_6$ is almost a pure chromium carbide, while M_7C_3 is more correctly reprenseted by $Cr_4Fe_3C_3$ and hence by the above carbide transformation the composition of the adjacent matrix zone is further changed. This may be represented in fig. 3 by a movement from line 2 towards line 3. It is also known (14) that the RT-permeability of the binary Fe-Ni-system has a minimum at

---

*[)] Any contribution from the carbides themselves to the change in magnetic permeability has not been considered here since measurements by ASPDEN et al. (2) have shown the M_7C_3 and $M_{23}C_6$ carbides (in Alloy 800) to have permeability values of 1.004, and hence can be neglected.

ca. 30% Ni and increases to a maximum at ca. 70% Ni. Hence the above carbide transformation may result in a further increase in μ (for a constant matrix volume). As indicated in fig. 6 it can be assumed, in a schematic way, that as carburisation proceeds, the $M_{23}C_6$-zone with permeability μ_1, moves at continuously increasing thickness into the material. The volume or thicknessof the M_7C_3-zone, have permeability $\mu_2 > \mu_1$, is also continuously increasing. Therefore the overall variation of magnetic response with time should be mainly determined by the rate of volume increase of the M_7C_3-zone. It has to be stressed that this is a very simplified model since SCHNAAS and GRABKE (10) have also shown that the metal composition of the carbides, both M_7C_3 and $M_{23}C_6$, and hence also of the affected matrix varies with distance from the surface as a consequence of the carbon concentration profile.

To assess the effect of carburisation on magnetic properties of FeNiCr-alloys it is therefore not sufficient to only deal with the penetration depth of the carbide zone(s) but rather to consider the resulting compositional changes of the matrix as a function of time and distance.

It should also be pointed out that in addition to the overall concentration gradient of the matrix across the carburised zone considered above, similar gradients may occur around each individual carbide precipitate - in particular at the internal front of the $M_{23}C_6$-zone where precipitate density is much smaller. These would give rise to corresponding magnetic effects as discussed above.

It should be further mentioned that the permeability values may be influenced by the distribution of the ferromagnetic phase because of demagnetisation effects in low fields. For a given volume fraction of ferromagnetic phase, connected particles would be expected to yield higher values of magnetisation than isolated particles. Hence it is expected that the carbide size and distribution (for equal amounts of carbon picked up) will also affect the change in magnetic response.

3. Experimental details

3.1. Methods of magnetic measurements

When a material of mass m and magnetic susceptibility χ is placed in a non-uniform magnetic field (H; $\delta H/\delta x$), a force in direction x is exerted on it according to

$$F_m = \chi.m.H.\delta H/\delta x \qquad (1)$$

This principle is being used in various experimental arrangements, set up to determine magnetic susceptibility values by gravimetric or dynamometric measurements.

In the FARRADY method, which is used in the present study, the sample is suspended from a self-compensating electronic microbalance into the air gap of a electromagnet preferably having poles of such a shape that the product H.$\delta H/\delta x$ remains constant over the entire space occupied by the sample to be measured thereby ensuring that identical forces are exerted on all elements, dm, of the sample. The total force, i.e. the sum of all elementary forces, influences the balance and can be measured. It is thus possible to assess all types of susceptibility and magnetisation up to saturation.

It is unnecessary to have a quantitative value for the product H.$\delta H/\delta x$ as this can be evaluated as an apparatus constant (C) by measuring a substance with known susceptibility - e.g. $MnSO_4 . 4H_2O$ with χ = 819.33 . 19^{-9} at 17°C - :

$$F_m = m \chi C \qquad (1a)$$

If the sample is further surrounded by a microfurnace and contained in a controlled environment (e.g. a double-walled water-cooled fused silica tube filled with inert gas or under high-vacuum), the variation of F_m with temperature can be recorded, i.e. the change in magnetic susceptibility with temperature and hence the Curie-temperature can be determined which may allow identification of the sample substance or of magnetic components of the sample.

The furnace assembly can also be substituted by a copper tube surrounded in the lower regions by a copper-coil through which liquid nitrogen is fed at a controlled rate enabling continuous temperature cycling between room temperature and ca. - 150°C. For better heat transfer the sample tube can be filled with pure helium.

Fig. 7 a-c explains the measurement principle and shows a view of the facilities used in the present study.

In addition, another method, based on the principle of RANKINE's balance was used. This may be considered as an inversion of the FARADAY method. Here a small permanent magnet is suspended from a self-compensating electronic microbalance above the sample to be assessed (fig. 8a). Again, the force acting on the magnet is propertional to the amount and magnetic strength of the material affected by its field. This method is somewhat more difficult to calibrate, i.e. to apply for measurements of quantitative data of χ or μ [*], therefore it is used mainly for relative measurements, i.e. to follow the variation of magnetic response of a single specimen with time (e.g. during carburisation), or to measure variation of magnetic response as a function of location on the specimen's surface (scanning). For the latter purpose the specimen or any other component, e.g. turbine blades (16), is mounted on a X-Y-table, which allows full assessment of the magnetic response over the entire surface, (fig. 8b).

By using a small hot/cold stage supplied form a thermostat/ cryostat it is possible to vary the temperature of measurement within a limited range (-50°C to + 200°C); the present measurements, however, were all carried out at room temperature.

It has to be taken into account however that the measured reponse signal is also a function of the distance between specimen and magnet since the magnetic field H and its gradient $\delta H/\delta x$ vary with distance from the poles of the magnet (see also App.).

---

[*] It also does not allow for determination of saturation magnetisation, i.e. the variation of χ or μ with magnetic field.

3.2. Test materials and carburising conditions

As the 25 chromium 20 nickel steels are the most widely used alloys within the petrochemical industry in Europe for cracker tubes and pipes, the major part of the present study has concentrated on this class of material. Table I gives the analysis of three materials used in these studies, i.e. HK 40 centrifugally cast tube, wrought AISI 314 type bar and a specially manufactured laboratory cast "model" ternary alloy which can be considered to be 55 Fe 25 Cr 20 Ni.

In addition a sample originating from a tube-section of an industrial naphtha cracker plant, made from centricast HK 40, was included in this investigation. The tube had been operating for 24 months at temperatures between 920 and 1025°C.

Coupons of standard size of 10 x 8 x 3 mm were machined from these alloys and carburised in H_2-CH_4-mixtures with carbon activities of 0.8 and 0.3, respectively, at all test temperatures, i.e. 825°, 925° and 1000°C. Table II gives the specific test conditions. Further details of the carburisation study are given in reference 7. After pre-determined exposures the specimens were removed from the carburisation rig and their change in weight and magnetic response measured. They were subsequently either re-exposed to the carbonaceous atmosphere or evaluated for changes in micro-structure and composition using the full range of structural analysis techniques (7).

Table I : Chemical composition of alloys used in the gaseous
carburisation test programme.

MATERIAL	FORM	CHEMICAL ANALYSIS – WT % ELEMENTS								Label of speci-mens
		C	Si	Mn	S	P	Ni	Cr	Others	
AISI 314	Wrought (Commercial)	0.06	2.04	1.12	0.006	0.023	20.30	24.07	Fe-Bal.	CSA
HK 40	Centri-cast (Commercial)	0.29	1.35	0.60	N.D.	N.D.	21.20	25.10	Fe-Bal.	CSB
'Model' 25-20-55 Alloy	Cast (laboratory)	0.01	0.04	0.10	0.005	0.004	19.87	24.55	Fe 55.56	CSC

Table II : Gaseous environments chosen to assess the carburisation
behaviour of the alloys in table I.

Composition-Vol. %	Carbon Activity (a_c)	Temperature (°C)	Pressure (bar/absolute)	Flow (litres/h)
1.22 % CH_4 – 98.78 % H_2	0.8	1000	1.6	6
4.39 % CH_4 – 95.61 % H_2	0.8	825	1.6	6
1.99 % CH_4 – 98.01 % H_2	0.8	925	1.6	6
0.45 % CH_4 – 99.55 % H_2	0.3	1000	1.6	6
1.74 % CH_4 – 98.36 % H_2	0.3	825	1.6	6
0.77 % CH_4 – 99.23 % H_2	0.3	925	1.6	6

4. Presentation of results

4.1. As-received condition

The study of the carburisation behaviour of 20 Ni 25 Cr-steel reported elsewhere (7) involved samples of the three alloys given in table I with different surface treatments. Measurements of the magnetic response of the materials in the starting condition using the Rankine-type balance are compiled in table III. The values reported are average values from measurements of the two major faces of 5 individual specimens of each materials.

Table III : RT-values of magnetic response of the alloys used for carburization studies as measured by the Rankine-type balance.

Alloy	180' grit		e-polished		machined
	3 mm *)	1 mm *)	3 mm *)	1 mm *)	3 mm *)
AISI 314 (CSA)	0.55 ± 1 %	5.51 ± 1 %	0.52 ± 4 %	5.15 ± 1 %	0.50
HK 40 (L) (CSB)	0.87 ± 17 %	7.62 ± 6 %	0.78 ± 15 %	7.19 ± 8 %	–
Mod.Alloy (CSC)	15.2 ± 20 %	171.2 ± 23 %	12.5 ± 18 %	146 ± 15 %	–

*) distance specimen-magnet

It is seen from table III that the wrought material AISI 314 and the cast alloy HK 40 (L) both show very low values, typical of those measured on austenitic paramagnetic materials. The values are approximately equal for both alloys and there appears to be no significant dependence upon surface treatment. Conversely the 20/25 Ni-Cr-model alloy shows relatively high values indicating the presence of a ferromagnetic phase. In the electropolished condition somewhat lower values have been found on this alloy than those recorded on '180' ground specimens, and a greater scatter between different

specimens and even between the magnetic response values of the two major faces of one and the same specimen was noticed.

It is proposed in particular that the slight ferromagnetism of the laboratory cast 'model' alloy may originate from structural or compositional heterogenities due to the casting and solidification process. These should disappear after long-term homogenisation annealing at elevated temperature. Fig. 9 shows the variation of F_m as measured on specimens of the alloys under consideration after annealing for various time intervals at 1000°C under high-vacuum. While alloys AISI 314 and HK 40 (L) do not show any change (even when measured at higher sensitivity, i.e. at 1 mm distance), the 'model' alloy exhibits a continuous decrease in magnetic response with annealing time. It was found that 50 hours at 1000°C had been insufficient to equilibrate the structure and hence the ferromagnetism did not completely disappear. A detailed study of this problem (17) revealed indeed the presence of (δ-) ferrite in the austenite matrix of this alloy and the development of σ-phase therefrom by annealing.

4.2. Carburised specimens

After exposure to a 0.8 carbon activity H_2-CH_4-mixture for 50 hr at 1000°C AISI 314 specimens showed a remarkable increase in F_m by ca. 100 units when measured at 3 mm distance at RT in the Rankine-balance. A scan of the magnetic response of the different faces of the carburised test coupon revealed strong fluctuations of F_m with the face considered and with the position on this face (fig. 10). From a typical scan across the major faces, A --> B and B --> A it was observed that the magnetic response reading had a minimum at approximately the centre of the specimen and increased towards the edges before falling again when approaching these. This behaviour can be explained by taking into account the magnetisation volume of the magnet and the typical carburisation pattern of the test specimens. The specimens carburise from all 6 faces, hence when the magnet is traversed towards the edges it not only "sees" the effect of the carburised top face, but it also reveals the effect of the carburised layer of the lateral face

(orthogonal to the scanned face)[*]. This is also explained by the schematic presentation in fig. 11. When the magnet is traversed over the edge of the specimen, the volume of ferromagnetic material rapidly drops causing the F_m to decrease. This is particularly evident from the scans on faces G/H and I/J (fig. 10).

Another feature evident from these scans is the fact that the response profiles are not symmetrical, i.e. it has to be concluded that the degree of carburisation, at least in terms of conversion of para- into ferromagnetic material, is not uniform over the whole specimen.

This is in agreement with fig. 12 a + b taken from the work of HARRISON and NORTON (7) showing the non-uniform variation of the volume percentage of carbides over the cross-section of different alloy specimens after various exposure periods.

Contributing factors to the non-uniformity observed in fig. 10 and fig. 12 may be experimental (fluctuations in either the gas flow condition or carbon activity of the environment or temperature) or material variables.

In addition the fact that the hole in the specimen increases the carburisation surface locally can explain the higher values always monitored around this part of the specimens [**].

The edge effect is once more demonstrated in detail in fig. 13. In the lower part of this figure, a scan along the top side of a single carburised specimen (N5) is shown, indicating the drop-off in F_m when approaching the edges. If however, this specimen is surrounded by two similar specimens, the scan reveals, first of all, generally higher values which are due to a summing up of the effects of the neighbouring

---

[*] Account must also be taken of the effect of the bottom face which contributes but at reduced efficiency due to the greater measuring distance ($\sim 1/d$).

[**] Also the specimen identification lables (put by spark writing) on one lateral face of the samples seemed to give rise to some enhancement of carburisation.

specimens to N5, and furthermore the F_m-values are now increasing towards the edges as would be expected from the fact that more carburised volume is available in these regions (see fig. 11).

Fig. 14 shows how scan profiles of F_m across the major face develop with increasing exposure to the 0.8 activity gas at 1000°C. It is seen that the overall level of F_m increases with time tending to achieve a constant value for longer times ($\geq$ 250 hr). In addition the non-uniformity and particularly the minimum at the centre disappears. This can be explained from the structural observation indicating that after 600 hr/1000°C/a_c 0.8 the specimens are almost completely through carburised (fig. 12a).

The magnetic-response scanning profiles appear therefore to be relatable, at least in a qualitative way, to the carbide concentration profiles reported in fig. 12, and it may be assumed that the minima of scan curves (figs. 10 & 14) indicate the presence of a less carburised core in the specimen.

It has been pointed out already (§ 2) that, because of the controlling C-diffusion process a carbon concentration gradient will build up as long as the specimen is not yet fully carburised and that carburisation will lead to a Cr-depletion of the matrix in the carburised zone due to the precipitation of Cr-rich carbides; thus a Cr concentration gradient towards the uncarburised core will develop.

During the elevated temperature post-exposure annealing of a partially carburised specimen, i.e. without further carbon access, these concentration gradients may tend to homogenise. Fig. 15a confirms that some diffusion must have occurred when a carburised specimen (50 hr/1000°C/0.8 a_c) was annealed for 50 hr at 1000°C in argon because the magnetic response became significantly reduced by this treatment.

Considering that a strong carbon concentration gradient exists after 50 hr/1000°C/0.8 a_c (see HARRISON et al. (7)), hence providing a big driving force for carbon inward diffusion, and that M_7C_3-carbides will readily dissolve at 1000°C when carbon is removed from the surrounding matrix, it is expected that significant inward diffusion of

carbon will occur during post-carburisation annealing of <u>partially</u> carburised specimens.

As a consequence of this carbon-diffusion the M_7C_3-carbides in the surface and sub-surface regions will tend to dissolve and thus supply Cr (+ Fe) back to the previously depleted matrix. This of course, causes the F_m to decrease as is shown in fig. 15a. The carbon thereby released will continue to diffuse towards the uncarburised centre of the specimen, where precipitation of $M_{23}C_6$ may occur.

It was indeed observed (fig. 15b) that the width of the $M_{23}C_6$-zone was increased by ageing by ca. 100 µm compared to the as-carburised state whilst the width of the M_7C_3-zone remained almost unchanged. It is also evident from fig. 15b that the M_7C_3-particles have significantly reduced in density and size (volume) by the soaking process.

From these results it cannot be excluded, however, that outward Cr diffusion driven by the Cr-gradient (e.g. fig. 4b) has taken place at the same time as inward carbon diffusion and contributed to the observed reduction of the magnetic response.

In any case, continuation of the soaking process of that specimen would have finally lead to an uniform carbide distribution over the whole cross-section with the final precipitation density depending upon the degree of pre-carburisation. On the other hand, when a through carburised specimen (600 hr/1000°C/0.8 a_c) was soked at 1000°C, the magnetic response remained unaltered due to the lack of any C or Cr-concentration gradient giving rise to diffusion/homogenisation processes.

4.3. Kinetic studies

In order to establish how the magnetic of 25/20 CrNi-steels with different structures and surface treatments developed with duration or extent of carburisation, a number of corrosion experiments were carried out at various temperatures (825°, 925° and 1000°C) and under

environmental conditions corresponding to 0.3 and 0.8 carbon activity. Figs. 16 to 18 show the respective changes in magnetic response as function of exposure time, each measured point of the various curves corresponding to an individual specimen exposure. Various conclusions can be drawn from these graphs :

i)   for both carbon activities (0.3/0.8 a_c) at 825°C the alloys CSA and CSB showed practically no change in F_m, except for CSB (alloy HK 40) which in 0.8 a_c gas in the electropolished surface condition showed a rapid initial incrase followed by a decrase upon further exposure (when measured at high sensitivity, i.e. at 1 mm distance),

ii) the model alloy (CSC), exhibiting a higher initial value compared to the other alloys generally showed a greater change in F_m [*)] during carburisation, in particular for the exposures at 825°C/0.8 a_c,

iii) this difference between the different alloys decreases with increasing temperature and carbon activity (fig. 19),

iv) under all exposure conditions alloy CSC generally exhibited a rapid increase of F_m up to values of ca. 300 followed by only a further slight increase with continuing exposure, whilst the other two alloys showed a more gradual increase (for T<1000°C, 0.8 a_c).

In many studies the degree of carburisation is generally measured by determining the amount of carbon picked-up by the material and since the magnetic response measurements were directed at monitoring the carburisation process non-destructively, an attempt was made to establish a correlation between the weight change data and the magnetic response values, (fig. 20 a-c).

In a general way it appears from the curves presented in figs. 16-20 that the F_m-measurements do reflect to some extent as do the

---

[*)] readings have been taken at 3 mm distance.

gravimetric measurements, the influence of the various parameters which control the carburisation process such as alloy composition and structure, surface condition, exposure temperature and carbon activity of the environment.

Referring specifically to the results presented in fig. 20 a-c, we can derive the following conclusions;

i)   the alloys CSA and CSB reveal at all temperatures in 0.3 a_c gas a smaller increase in F_m than for the same weight gain achieved in a 0.8 a_c-environment. At 825°C for both activities these alloys exhibit a very small, rapid increase in F_m (with onset of carburisation) which then, however, remains practically constant during further carbon uptake;

ii)   Independent of gas activity at 825°C the model alloy CSC for a given weight gain shows the same magnetic response;

iii)   this feature is also the case for this alloy when carburised at 925°C although the initial weight gain at 0.3 a_c seems to give rise to a somewhat smaller increase in F_m that at 0.8 a_c. This trend is more pronounced at 1000°C where the curve for 0.3 a_c clearly lies below that of 0.8 a_c – at least up to weight gains of 20 mg/cm^2;

iv)   with increasing temperature the curve for CSB at 0.8 a_c is approaching that of CSC.

These observations appear to indicate that for these alloys of nominally the same base composition (Fe, Cr, Ni-levels) the uptake of a given amount of carbon will induce, rather different types of Cr-depletion depending upon temperature. This could be due to either different C-diffusion or Cr-back-diffusion rates. It may be postulated that if carbon is diffusing more rapidly into the alloy (or conversely outward diffusion of Cr is rapid) the extent of maximum Cr-depletion at the surface would become smaller and retained in a narrower surface zone. A further consideration is that it is not the amount of carbon taken up during carburisation alone that determines the change in F_m, but

that the carbon initially present in the alloy will also have combined
with a certain amount of Cr. Hence, if a low C (e.g. CSA) or carbon-free
alloy (e.g. CSC) absorb the same amount of carbon during carburisation as
that measured for a carbon-containing alloy (e.g. CSB), the latter alloy
will be integrally more depleted in Cr than the former ones and should
therefore exhibit a greater magnetic response. This is indeed observed in
fig. 20 a-c, and it might be one reason for the fact that for the alloys
compared in this work the same weight gain may be associated with
different magnetic response values. Apart from this, other factors such
as the presence of minor alloying elements (e.g. Si), carbide size and
distribution or long range diffusion or alloying elements may play a role
as well.

4.4. Variation of magnetic response with depth of carburisation

The carbon concentration and thus the carbide vol. % of a
carburised material prior to through-carburisation decreases with
distance from the surface and therefore the residual matrix composition
will vary correspondingly. An attempt was thus made to explore the
variation of F_m with the carburisation profile. For this purpose on a
specimen of AISI 314, previously carburised for 264 hrs at 1000°C in
0.8 a_c gas, layers of controlled thickness were removed from one
carburised side by repeated grinding, and the magnetic response of the
remaining material was measured. As can be seen in fig. 21a, the magnetic
response of the stepwise ground face decreased in a continuous fashion
until at ca. 800 μm a steep decrease was observed followed by a further
continuous decrease (bottom curve of fig. 21a). This curve principally
reflects two features : first, it confirms that the magnetic response
decreases with increasing distance of the surface from the magnet, and
secondly it also shows that the magnetic response of the inner carburised
regions is smaller.

To compensate for the distance effect, the measured values were
corrected for a constant distance of 3 mm between magnet and actual
sample surface which yielded the middle curve in fig. 21a. Here it can be
seen that the removal of the first ± 300 μm of carburised material has
very little effect on F_m from which it can be concluded that this zone

consists of material with a constant (high) permeability. Further this curve again shows very clearly the sudden drop to an almost constant value after grinding down to ca. 800 μm.

The readings obtained after each grinding operation on the opposite face (S_2 top curve in fig. 21) showed between 0 and X_o only a very slight decrease reflecting the reduction of ferro-magnetic material on side S_1 while after removal of $X > X_o$ again a sudden drop was observed. These features can be interpreted in the following way : since all 6 faces of the specimen had been carburised, the reading taken on one face is the sum of the effect of this side measured at 3 mm distance plus the contribution of the opposite side at a distance 3 mm + $d^{*)}$ and that of the lateral faces.

Further it was observed from the microsection of the specimen in fig. 21 b that the specimen was almost completely through-carburised i.e. all carbides are already of the M_7C_3-type even though the carbide vol. % in the middle of the specimen had not yet reached the same level as that found within the surface regions. This leads directly to the assumption that the Cr-depletion induced by the carbide precipitation had lead to the development of a ferromagnetic layer (shell) with an inner core underneath which, although being carburised to a certain extent, exists a non-ferromagnetic austenite matrix (i.e. still containing a sufficiently high level of chromium). Therefore the reverse side (S_2) is also magnetically coupled to the front side (S_1) underneath the magnet by the lateral sides, increasing thereby the contribution of S_2 (and vice versa). Grinding back side S_1 to the non-magnetic core (X_o) has the effect of bringing $F_m(S_1)$ to zero and to disrupt the coupling of S_2 to S_1. It is proposed that this causes the step decrease of F_m at X_o recorded in both the measurements made from S_1 and S_2. Beyond X_o the readings on S_1 are due to the effect of the carburised zone S_2 at the distance 3 mm + Δd whilst the readings on S_2 give a higher value because of the smaller measuring distance (3 mm). The small decrease found for $X > X_o$ on side S_2 is probably due to the removal of carburised material wit continued grinding from the side faces, which still are in magnetic contact with the side S_2.

$^{*)}$ d = sample thickness

A similar exercise was carried out on a HK 40 sample from a cracker furnace tube which had been operating for 24 months at temperatures around 1000°C. Fig. 22 a shows the microstructure of the specimen and in fig. 22 b the variation of F_m with stepwise removal of carburised material from the inner tube side is plotted. The magnet-sample distance was always kept constant at 3 mm, and it was noticed that as for the middle curve of fig. 21 a, the removal of the first ca. 2 mm does not appreciably alter the value of F_m. Beyond this depth the magnetic response decreases rapidly with further material removal, reaching at ca. 4.5 mm the value for the uncarburised material.

The F_m-decrease measured when grinding back from the external tube surface has to be associated with the severe oxidation effects leading to noticeable Cr-depletion in the subscale region (see below).

An attempt was made to also monitor the composition of the residual austenite across the tube section of this sample, and the results are shown in fig. 22 c. It becomes evident therefrom that apart from a thin layer of Fe-enrichment at the inner surface, which probably again is associated with oxidation (see fig. 22 a) the iron content increases and the nickel concentration decreases with depth to ca. 2 respectively 4-5 mm. It was interesting to note however, that Cr shows a strong depletion gradient over the whole cross-section and appears never to reach the original bulk alloy concentration (25 %). This can be considered as evidence for the significant partitioning of this element in the carbide formation process. Also in the outer regions of the sample where virtually no carburisation had taken place, the Cr content was low. Therefore it can be assumed that Cr had diffused into the heavily carburised zone and/or had been consumed by the oxide formation at the outer surface (see fig. 22 a).

From fig. 22 b + c it can be further seen that F_m stays high and constant over approximately the same distance (ca. 2.5 mm) where the Cr-level is low (ca. 4 %) and almost constant. Over this same distance, the Fe-level is continuously increasing from about 53 % to ca. 63 % which indicates a significant (and varying) partitioning of this element into the carbides of this zone. On basis of these findings the carbide

precipitates of the first 2-2.5 mm zone may be considered to be of the $(Cr, Fe)_7C_3$-type.

4.5. Thermomagnetic analysis of a carburised alloy

As pointed out in § 2 the determination of the Curie-temperature of a carburised specimen should allow an estimation of the composition of the residual austenite, and eventually of the extent of carburisation.

Fig. 23 a shows an example of such a measurement on a HK 40 sample which had been exposed at 1000°C for 600 hr to a 0.8 a_c environment. It can be seen that the material is characterised by a rather steep transition from a ferro-magnetic to non-magnetic state revealing a Curie-temperature ($T_{c \, max}$) of ca. 240°C. The shape of this curve confirms the gravimetric results and the metallographic observations i.e. that this particular specimen was almost uniformly through-carburised to the maximum carbon level. If this was not the case a much broader temperature range for the transition from ferro- to paramagnetic behaviour would have been observed.

Taking into account relevant literature (12, 13) on the variation of Curie-temperature with alloy composition shown in fig. 23 b, it can be first of all anticipated that the Cr-level of the residual austenite of this specimen must be below 12 % with a Ni-content ranging between about 33 to 50 % (with corresponding Fe-contents). Furthermore, assuming a residual Cr-content of 5 %, then from fig. 23 b, a Ni-content of ca. 40 % can be derived for the residual austenite. This is in very reasonable agreement with the EMP-analysis shown in fig. 22 c which indicated that the austenite of the outer zone of a heavily carburised HK 40 tube had a composition of ca. 5 % Cr 40 % Ni 55 % Fe. This finding also confirms line 3 of fig. 3 which indicates the compositional change of the austenite under the assumption of $Cr_4Fe_3C_7$-precipitating during carburisation.

5. Discussion

The present results obtained on materials from the 25Cr-20Ni class of
alloy confirm that carburisation alters the magnetic properties of
FeCrNi-steels and that hence magnetic techniques can potentially be used
for (continuous) ND-monitoring of the carburisation process. Although the
magnetic susceptibility/time-curves appear to reflect the kinetic
behaviour of these materials including the influence of carbon activity,
temperature and specimen surface finish on the carburisation process, and
in-depth analysis shows that the rate of change in magnetic response is
not equivalent to the rate of carbon pick-up. This is particularly
evident from the F_m vs Δ C/A-curves, where for different alloys the same
account of carbon pick-up may induce quite different F_m-changes. This is
not surprising since it is not the carbon or carbide precipitation which
is directly responsible for the change in magnetic properties, but rather
the related change in composition of the residual austenite.

Carbide formation ($M_{23}C_6$ or M_7C_3) primarily involves chromium
consumption from the alloy and causes thereby the affected alloy zone to
become ferromagnetic by raising the Curie-temperature of the residual
austenite above room temperature. This is also the reason why in high
Cr-alloys such as 50Cr50Ni, carburisation is not associated with a
noticeable increase in magnetic susceptibility (20), since the carbide
formation does not bring the Cr-concentration down to a level where the
alloy becomes ferromagnetic at RT. The alloy can absorb and precipitate a
lot of C before the chromium level of the remaining matrix is
sufficiently reduced for it to become ferromagnetic.

The most important question remaining is, what do the changes in
magnetic susceptibility represent since, as already stated, these
magnetic changes cannot be unequivocally correlated with the amount of
carbon picked up by the material ?

The overall carburisation process is determined by the rates of
absorption and subsequent inward diffusion of carbon and the rate of
reaction of this carbon with carbide forming elements to precipitate
carbides, each of these processes being dependent in a specific way on

temperature, activity of the environment and alloy composition. It is reasonable to assume that the actual carbon resp. carbide distribution and hence the type of resulting Cr-depletion will be dependent upon these interrelated processes and most likely to be different for the same amount of carbon picked up (at different temperatures or by different alloys), giving rise to different F_m-values. When carbon is absorbed by the material it will tend to diffuse to the inner, lower carbon containing regions of the specimen and at the same time precipitate in the form of $M_{23}C_6/M_7C_3$ carbides. The relative rate of these two processes will determine the shape of the carbide/carbon profile and also the extent of corresponding chromium-depletion of the residual austenite. It is obvious that the rate of the two processes, excluding the influence of the carbon activity of the environment and temperature, will be dependent on alloy composition and structure, i.e. availability of carbide forming elements. It follows therefore, that the rate of increase in F_m should in some way reflect the rate of Cr-depletion due to carbide precipitation. Thus the initial slope of the F_m vs time curve will be smaller when either the rate of carbon uptake is low and/or inward diffusion of carbon is high.

The observation that the magnetic susceptibility of all alloys under all the conditions of exposure studied here, sooner or later reach the same constant value, may be explained in various ways. The first consideration is that as the carburisation front progresses into the material, away from the magnet, respectively into a lower field gradient area ($\delta H/\delta x$), the newly developping ferromagnetic layers will contribute less and less to the overall value. A further considation is that the F_m only increases until the maximum Cr-depletion (which may be equivalent to the maximum C-concentration) has been built up in the surface region. Data to confirm this are not yet available.

It is useful in this context to make reference to results on microstructural aspects of carburisation by E. Bullock et al. (19). In fig. 24 the correlation which these authors have established between gravimetric and metallographic estimation of carburisation attack for the same 25/20 CrNi-steels is shown. Comparison of these curves with the results in figs. 16-18 and 20, shows that in terms of time-dependence at

825°C the F_m-curves appear to match much better the weight change curves than the plot of maximum carbon penetration versus time. It can be seen that at this temperature the rate of carbon uptake for alloy CSC is much higher than for CSA & CSB but it is also observed that a certain amount of carbon was precipitated in alloy CSC in a much narrower region than in CSA or CSB. It is proposed that this is due to the fact that the rate of C-uptake in the latter alloys is greatly reduced because of the presence of a SiO_2-layer. The absorption rate of carbon is limited by the presence of this SiO_2-layer and therefore diffusion of carbon that has actually been accepted by the material occurs to a greater depth and thus the local chromium depletion (and hence change in magnetic susceptibility) is not as severe as in alloy CSC. Conversely, since CSC has no protective SiO_2-layer, the rate of C-uptake is much greater, leading to a greater C-supersaturation in the surface zone, hence favouring carbide precipitation and Cr-depletion, i.e. increase of F_m.

By comparison of the results at 925°C, in fig. 24 and 17, it can be seen that the magnetic susceptibility/time-curves are in much better agreement with the penetration curves than with the gravimetric results, e.g. CSB and CSC show almost the same F_m-behaviour even though their respective weight gains are quite different. Further, this comparison shows that the weight gain (or time) necessary to achieve complete penetration corresponds to that at which the maximum F_m-value is observed. This is also the case for the 1000°C results.

Thus, on one hand it can be postulated that for exposures at 925°C and 1000°C, where SiO_2 ceases to have a significant effect on carburisation (at least for CSB), the time to reach F_{max} is determined by the carbide precipitation front having reached the centre of the specimen. At 825°C, CSC reaches the same maximum value of F_m (ca. 300) but at a much smaller depth of penetration (or less weight gain). This again is conceivable since at this temperature diffusion rates are lower and precipitation may become predominant. Therefore the carbon picked up is precipitated in a relatively narrow subsurface zone which consequently becomes severely depleted in Cr resulting in high F_m-values.

In conclusion, it is proposed that the achievement of F_{max} corresponds with the attainment of maximum Cr-depletion of the outer layer. This may or may not coincide with the time at which through-carburisation of the specimens used here has occurred. It follows that if F_m has not reached its maximum value, the carbon surface concentration (and thereby Cr-depletion) has also not attained its maximum value, and probably the carburisation front has not yet reached the centre of the specimen. Thus, if for the same weight-gain one of the present alloys has reached F_m and another has not, then this would indicated that in the latter case carbon inward (and/or Cr outward) diffusion is higher than for the former alloy.

6. Conclusions

The results of the present study can be summarised in the following way :

1. Carburisation of Cr-Ni steels affects the magnetic properties of the material. When using magnetic techniques for non-destructively monitoring the progress of carburisation in such steels, it must be remembered that the change in magnetic response of the material is due to compositional alterations of the matrix of the carburised zone, i.e. due to alterations of the ration of ferromagnetic to non-magnetic elements resulting from the precipitation of Cr-rich carbides. Hence there is no direct relationship to the carbide vol.% or carbon content (i.e. weight gain) of the sample to be expected.

2. It is proposed that the general character of the observed magnetic susceptibility/time relationship is determined by the following features :

   - the initial rate of F_m-increase is determined by the carbon pick-up and resulting carbide precipitation respectively matrix depletion within the surface-close region;

   - the further development of F_m is determined by the way the carburised ferro-magnetic zone grows beyond the "reach" of the used

magnet monitor system which had only a limited field strength. It appears that F_m continues to increase as long as the Cr-concentration within a limited surface zone is decreasing whereby the permeability of this zone is increasing. It is proposed that when the maximum possible C-concentration (thus Cr-depletion) has been achieved within this zone (ca. 4 wt.% C for 25/20CrNi-alloys at 0.8 a_c), μ and hence F_m become more or less constant. Further ingress of carbon and progress of the carburisation front does not appear to significantly increase the F_m-signal;

- in addition, the formation of the first layer of ferromagnetic austenite occurs at the closest distance to the magnet and has therefore the greatest effect. With progress of the carburisation front, the equivalent transformation will occur at a steadily increasing distance from the magnet, thereby having a reduced effect on F_m.

  When monitoring for example a carburised cracker tube from outside, this effect would be just the opposite, since the carburising front would be approaching the magnet, i.e. giving a steadily increasing effect, (magnetic material under a non-magnetic shell of decreasing thickness). In practice; in this case, a further complication results from the oxidation/nitridation effect of the outside tube wall close to the magnet, which will cause a F_m-signal of its own. A solution would be the removal of this scale and subscale surface before each monitoring test;

- it is anticipated that by using a magnet with a greater field strength the range by which the progress of depth of carburisation is monitored could be extended.

3. The ferromagnetic response for a given C-pick-up was noticeably dependent upon the composition and structure of the alloy, and for wrought alloys generally smaller increases of F_m (for same weight gains) were found.

4. It further became evident that the depth of carburisation and hence
   the type of Cr-depletion, will depend on the kinetics of carbon
   absorption, carbon diffusion and carbide precipitation. For high
   Cr-alloys most of the absorbed carbon will be retained in a narrow
   surface layer, in the form of chromium rich carbides (e.g. Cr_3C_2 for
   50Cr50Ni), while for lower Cr-alloys the same amount of carbon will be
   distributed over a greater distance.

5. Although a quantitative monitoring of the progress of carburisation,
   especially of different alloys, appears to be difficult, magnetic
   techniques are a rather convenient means of checking relative local
   fluctuations in the extent of carburisation on a particular sample.

6. It has further been shown by the present measurements that annealing
   of a partially carburised specimen brings about a partial restoration
   of the magnetic response (paramagnetic behaviour of the alloy) by
   homogenisation of the carburisation effects.

References

1. Krikke, R.H., Hoving, J., and Smit, K., Corrosion/76, Int.
    Corrosion Forum, March 1976, Paper 10.

2. Aspden, R.G., Economy, G., Pement, F.W., and Wilson, I.L.,
    Metallurgical Transactions, 3, (1972), 2691.

3. Swales, G.L., Rev. Int. Htes. Temp. et Réfract., 13 (1976), 146.

4. Ruziska, P.A., and Bagnoli, D.L., Ammonia Plant Safety 16 (1975),
    10, AlChE-Publication.

5. Orbons, H., DSM, Private communication.

6. Boogaard, J., Janssen, G.J., Van Wensch, P., DSM, private
    communication.

7. Harrison, J.M., Norton, J.F., in "Proc. Int. Conf. Behaviour of
    HT-alloys in aggressive environments", Petten 1979, p.661.

8. Bühler, H.E., Rahmel, A., and Schüller, H.J., Arch. f. Eisenhow., 3
    (1967), 223.

9. Grabke, H.J., Gravenhorst, U., and Steinkusch, W., Werkstoff u.
    Korrosion, 27 (1976), 291.

10. Schnaas, A., and Grabke, H.J., Werkstoff u. Korrosion, 29 (1978),
    635.

11. Bozorth, R.M., "Ferromagnetism", ed. D. van Nostrand, Comp. Inc.
    Princeton, New Jersey (1968).

12. Chevenard, P., Mém. Soc. Ing. Civ. France, 104 (1951), 1.

13. Jackson, L.R., and Russel, H.W., Instruments 11 (1938), 80.

14. Mathieu, K., Arch. f. Eisenhw. 16 (1943), 415.

15. Chevenard, P., C.R. Acad. sci. <u>198</u> (1934), 1149.

16. Lang, E., and Franck, F., Techn. Note P/07/79/32, (1979).

17. Lang, E., and Tottle, L., unpublished work.

18. Hubert, R. and Thuillier, J., private communication Acieries du
     Manoir Pompey, March 1975.

19. Bullock, E., Frampton, P.D. and Norton, J.F.
     "Structural aspects of gaseous carburisation of austenitic steels".
     Techn. Note P/84.81/1, Feb. 1981.
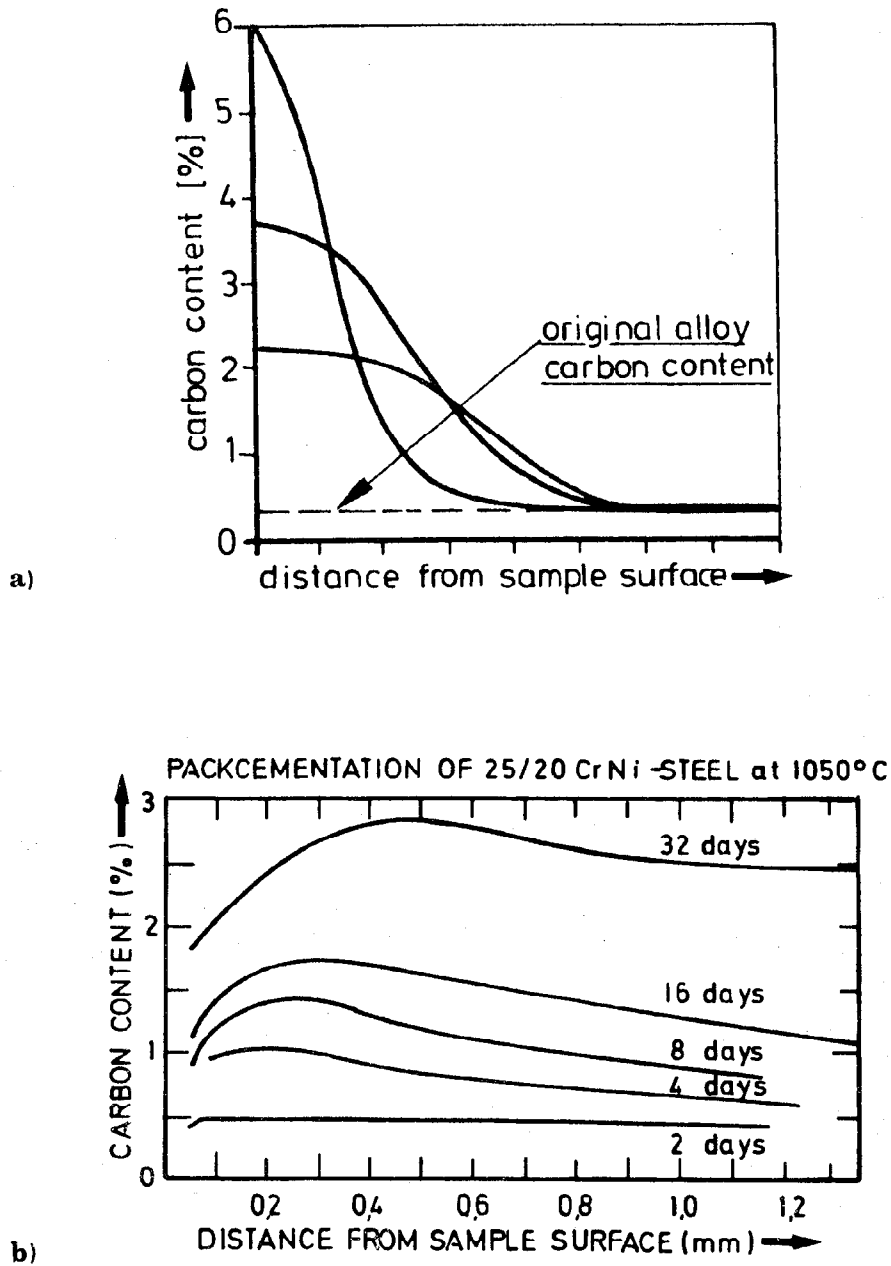
Fig. 1   a) Examples of possible carbon gradients in different carburized austenitic steels.

          b) Variation of carbon profile as a function of time of carburization (18)
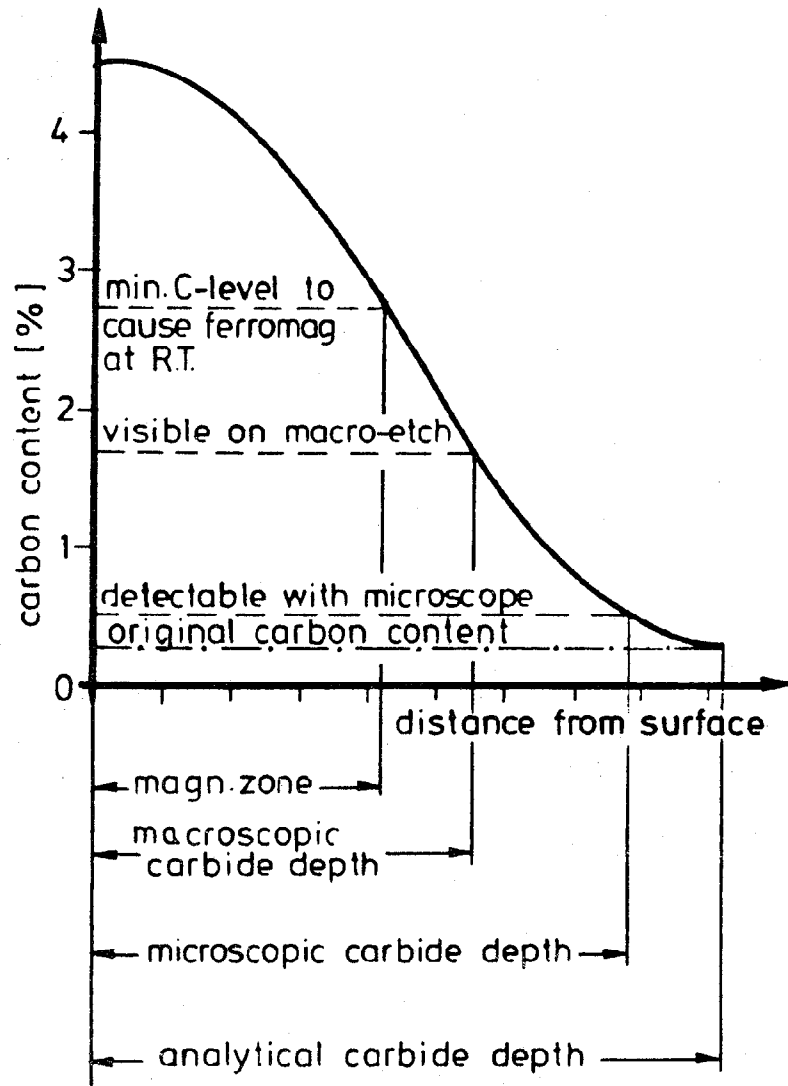
Fig. 2   Model of a cross-section of a carburized sample showing different
detection limits.
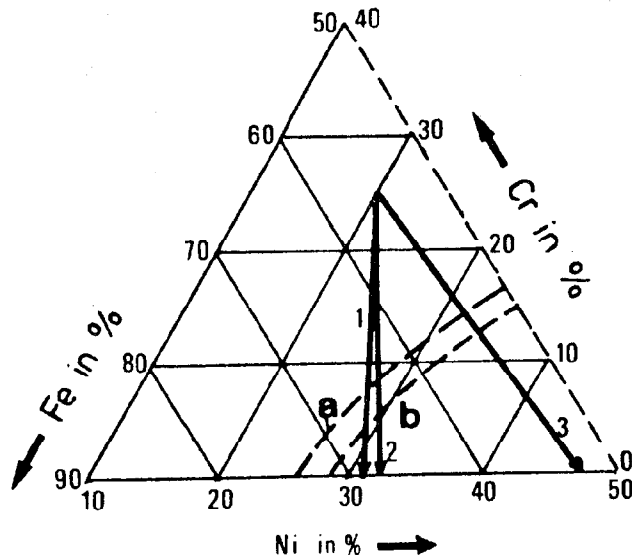
1 M_7C_3 with 2Fe-atoms
2 $M_{23}C_6$ " 8Fe- " } STEEL X 10 Cr Ni 2520
3 $M_7 C_3$ " 4Fe- "

a = -50°C | Curie temperature of the
b = +50°C | austenite (after P. Chevenard[12])

Fig. 3   Change in composition of the austenite matrix of a 25Cr20Ni-steel by Cr-depletion resulting from carbide precipitation during carburization (after 8).
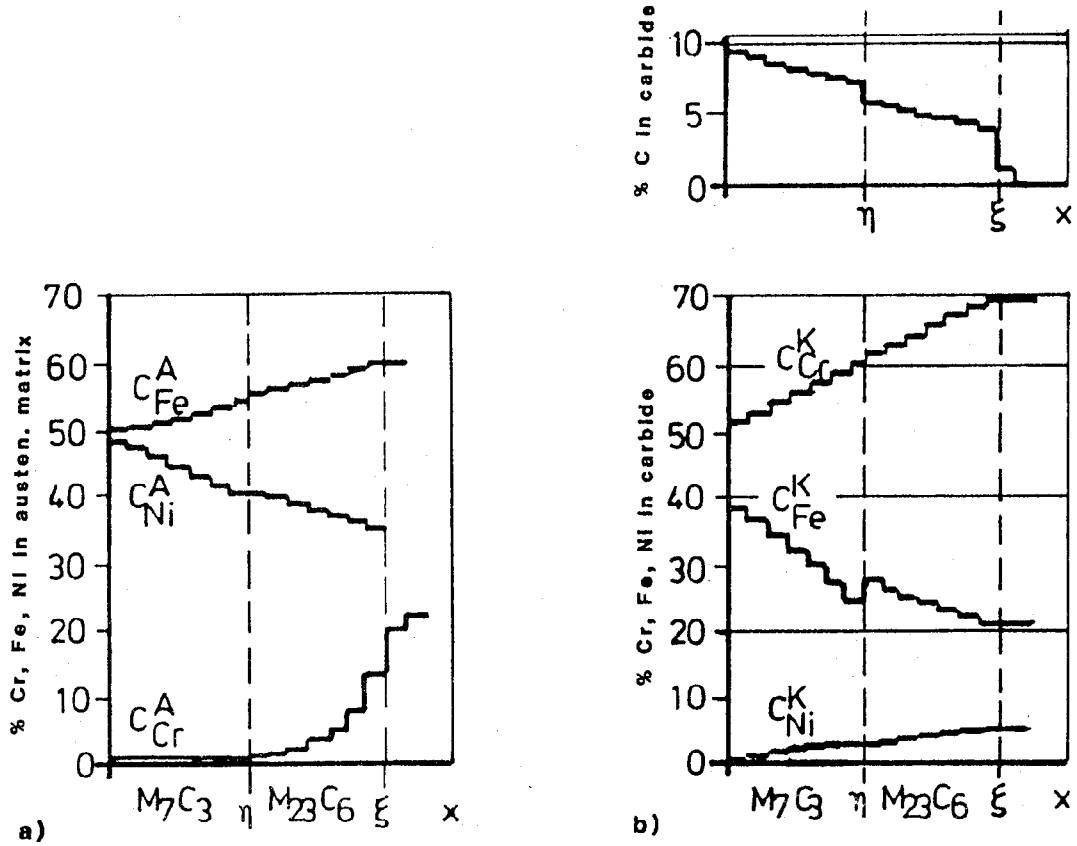
Fig. 4: Variation of composition of austenitic matrix (a) and of carbides (b) with depth in a carburised Alloy 800H sample (after 10).
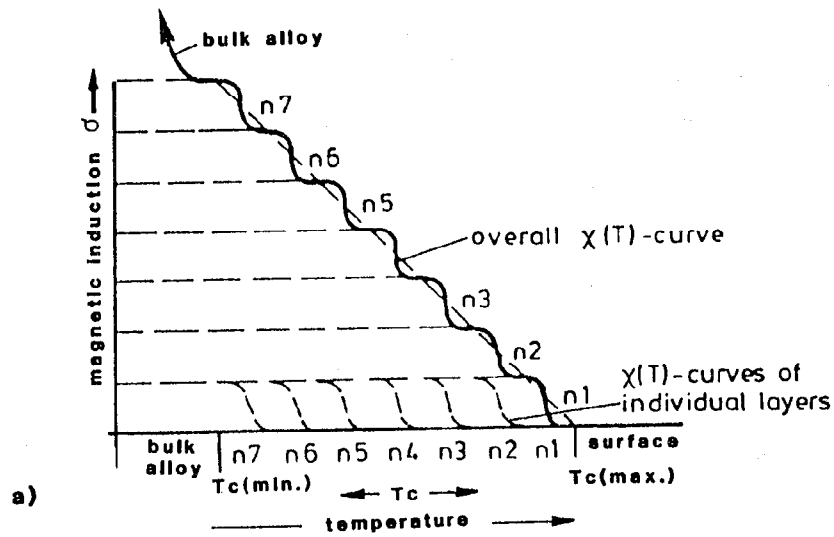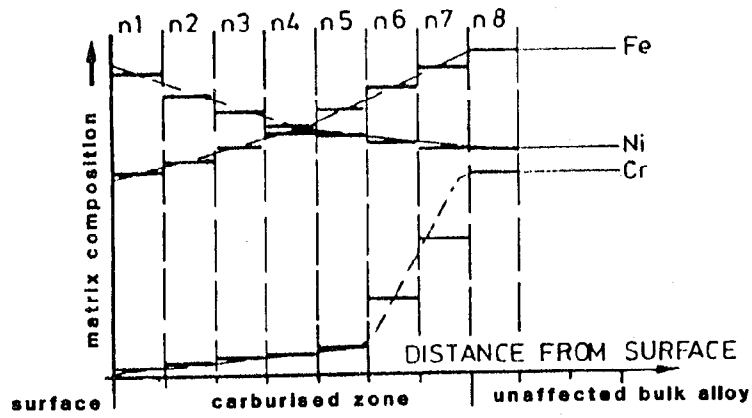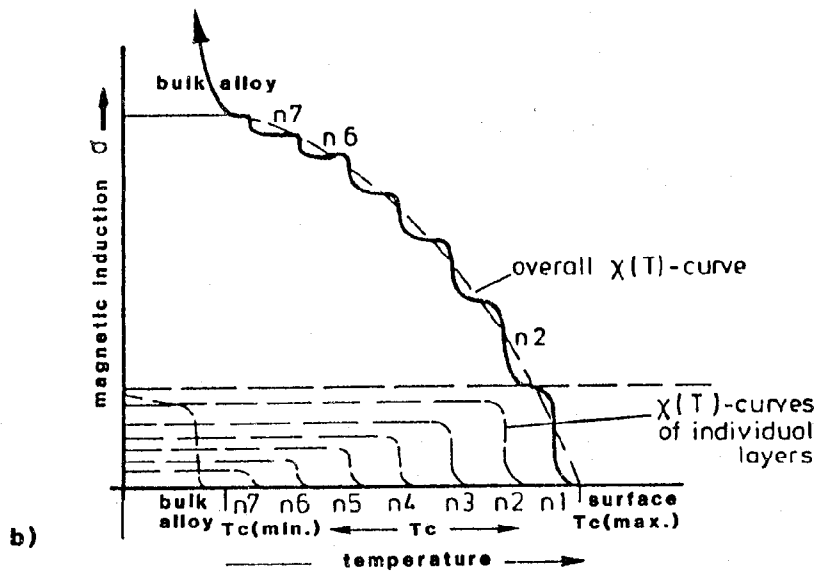
Fig. 5   Schematic presentation of matrix element concentration profiles of carburized
alloys and resulting temperature-magnetization curve.
a)   assuming alloy composition alteration only to affect T_c
b)   assuming alloy composition alteration to affect both T_c and μ

36
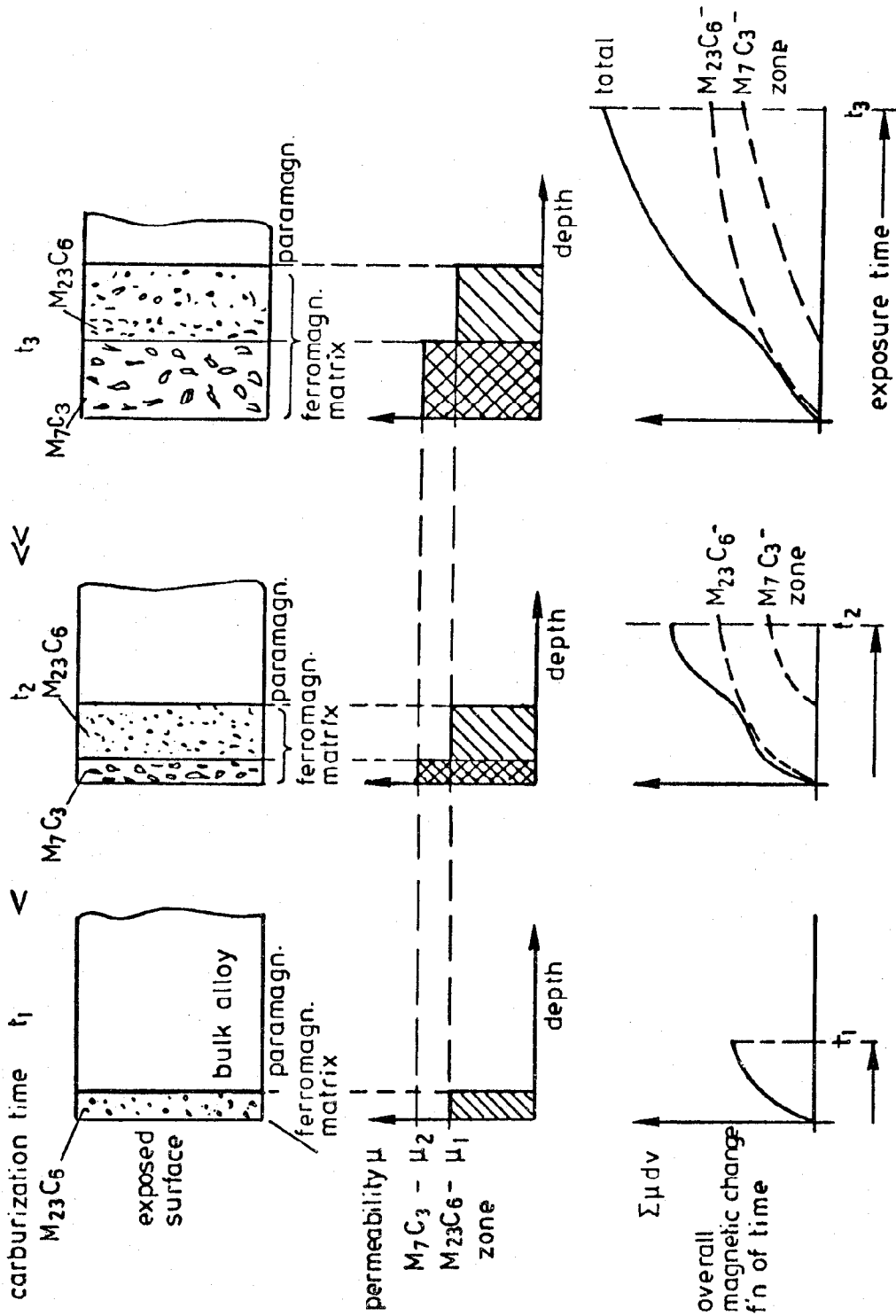
Fig. 6   Schematic presentation of progress of carburization and related increase of magnetization.
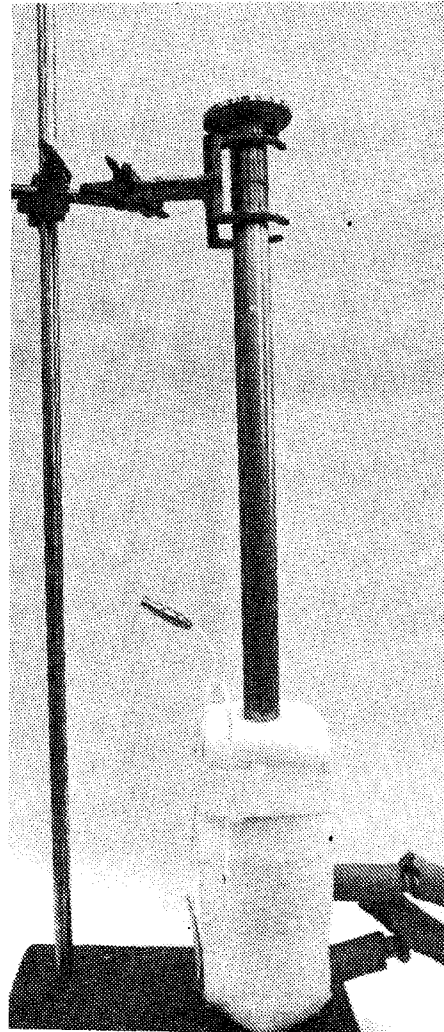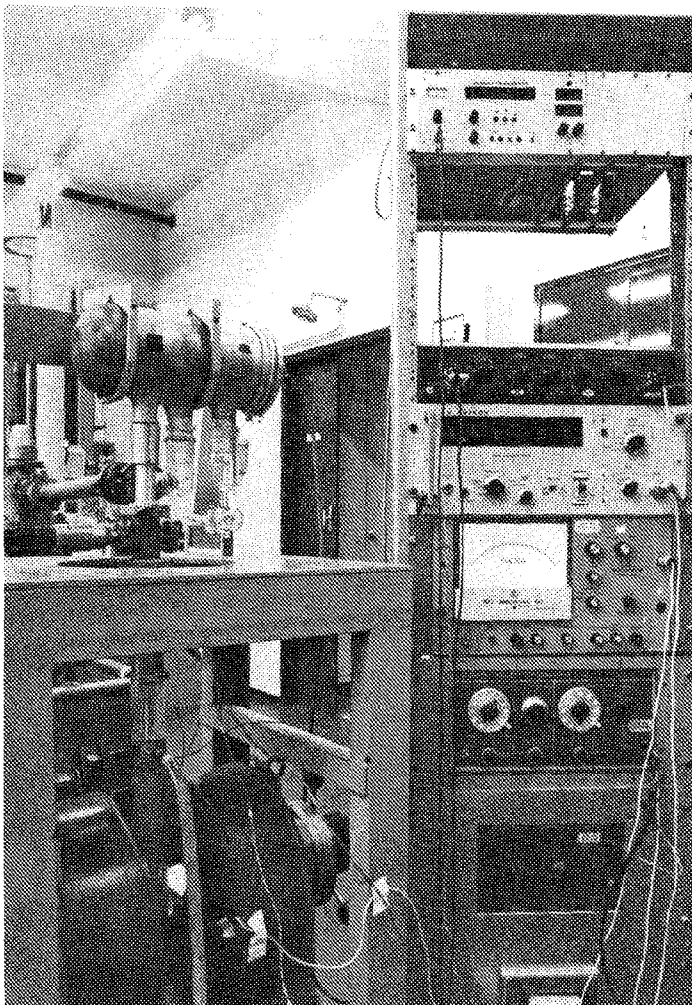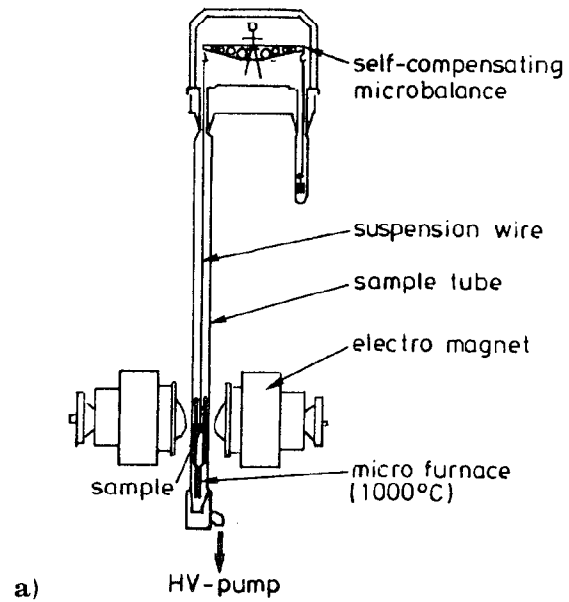
Fig. 7

a) Principle of Faraday-method for
   for measurement of
   susceptibility vs. temperature
b) View of the laboratory
   experimental HT-facility
c) LT-extension of laboratory
   facility.

self-compensating
microbalance

permanent
magnet

sample

hot/cold stage

movable xyz-support

a)

hot/cold stage
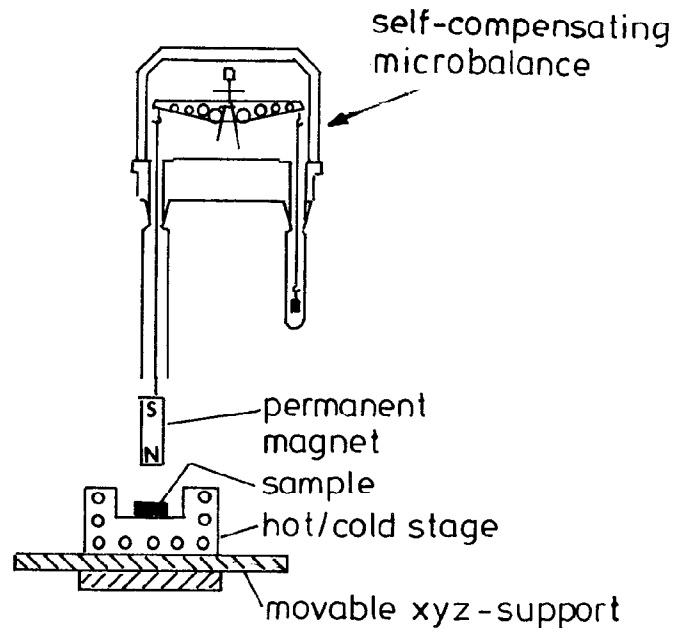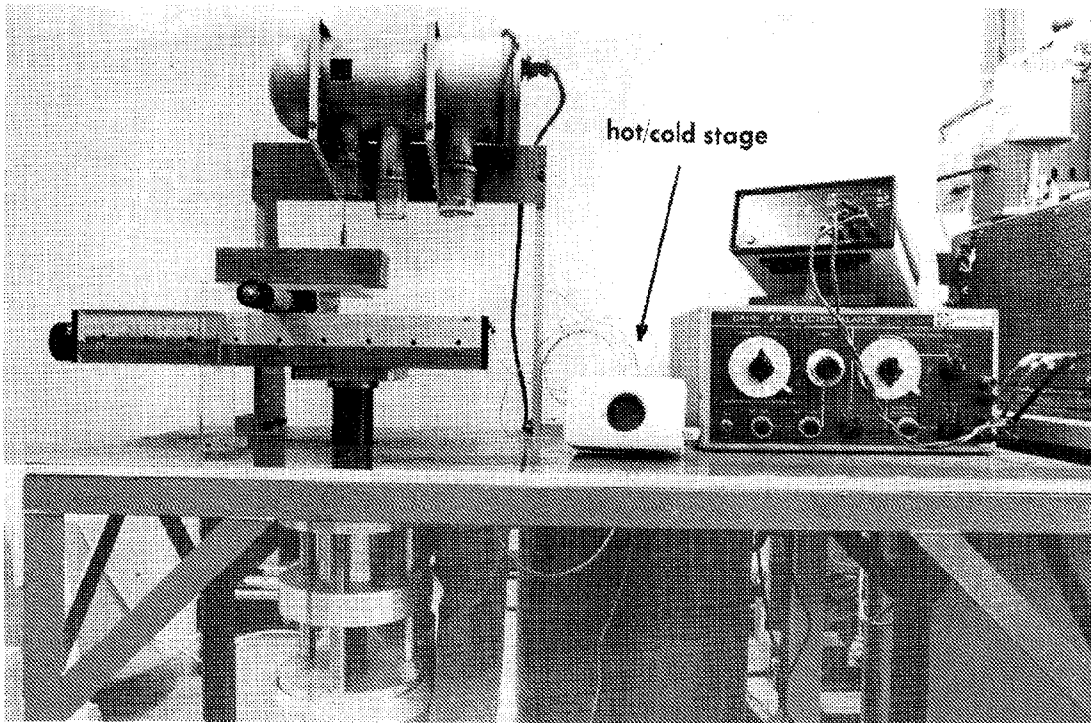
b)

Fig. 8   a) Principle of the RANKINE-method
          b) View of the laboratory Rankine-type balance.
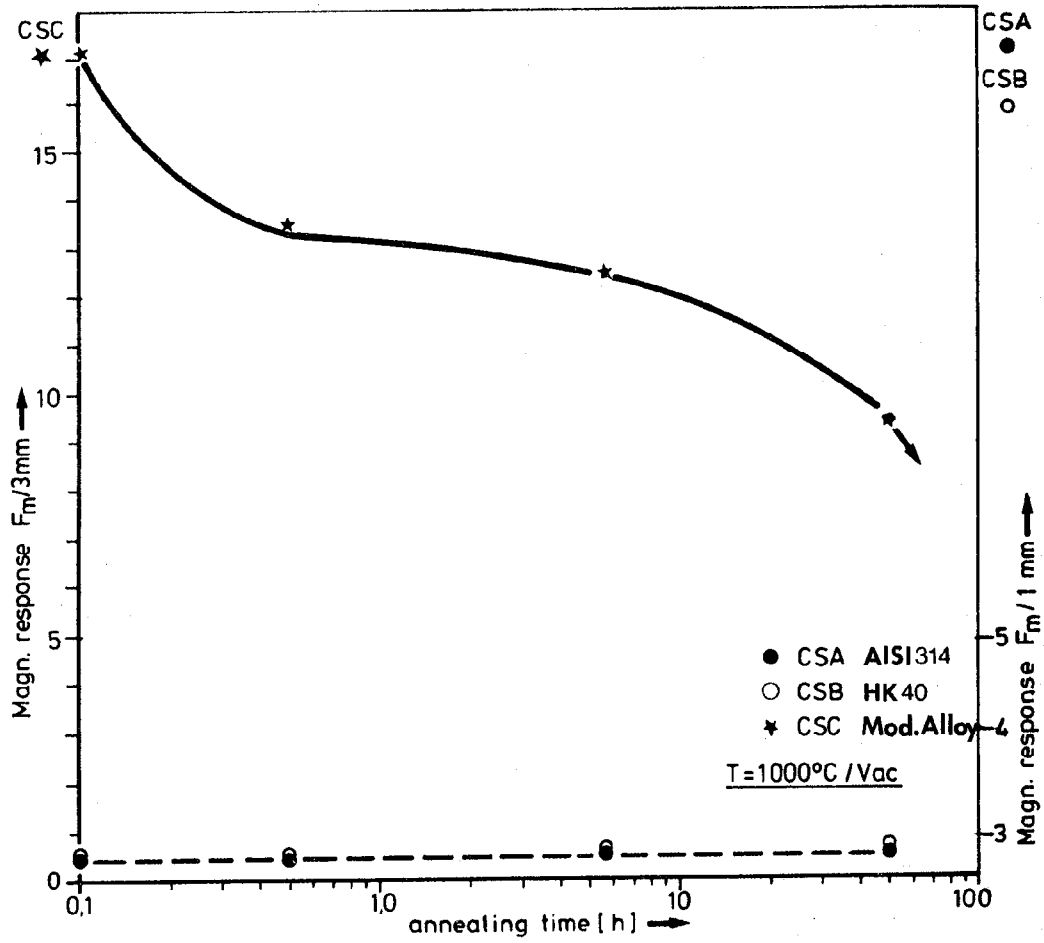
Fig. 9   Change in magnetic response during annealing of 20/25 NiCr alloy samples
in their initial state at 1000 °C under high vacuum.
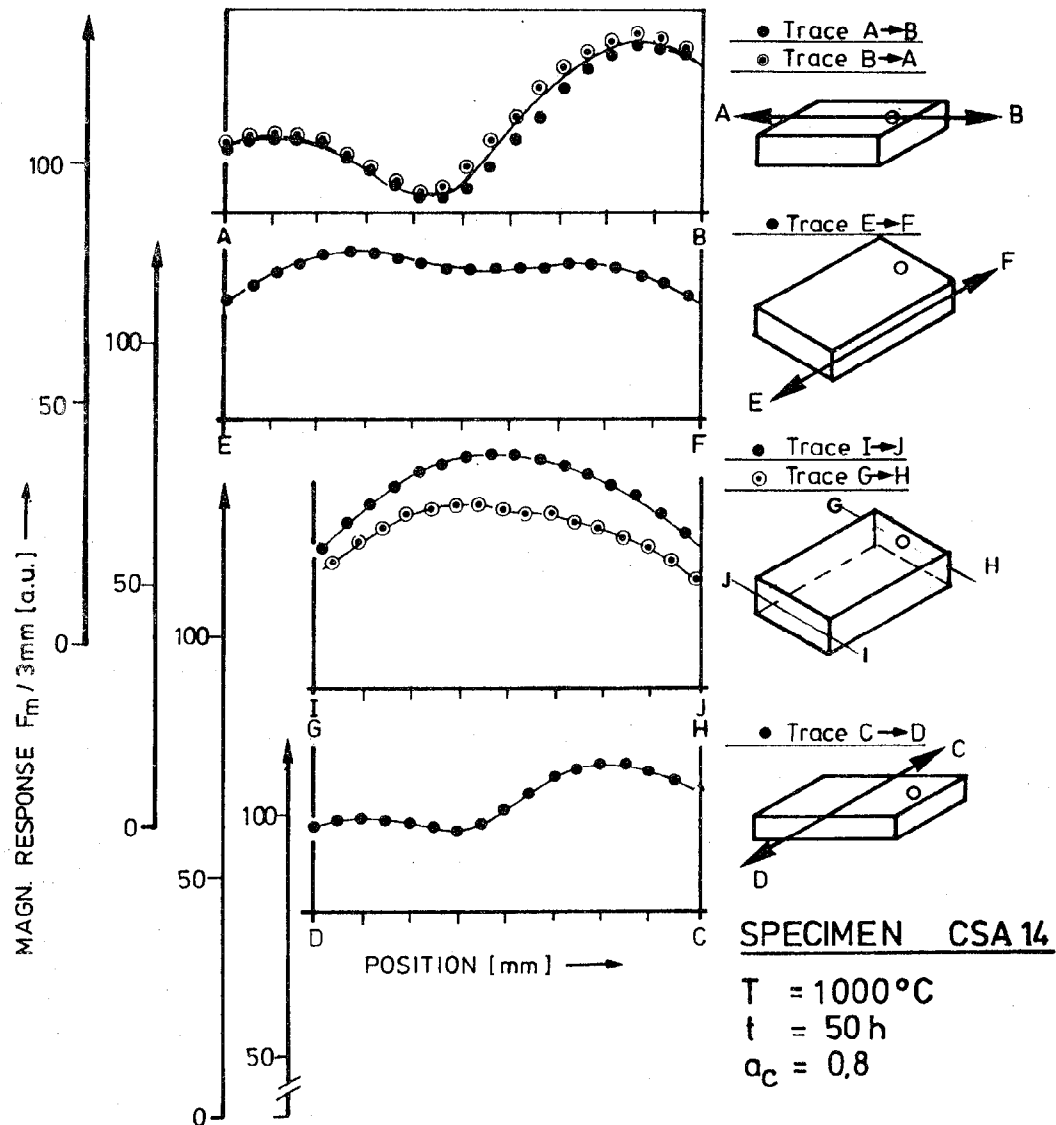
Fig. 10   Scan of the magnetic response of the different faces of an AISI 314 specimen
carburized for 50 hr at 1000 °C ($a_c = 0.8$).
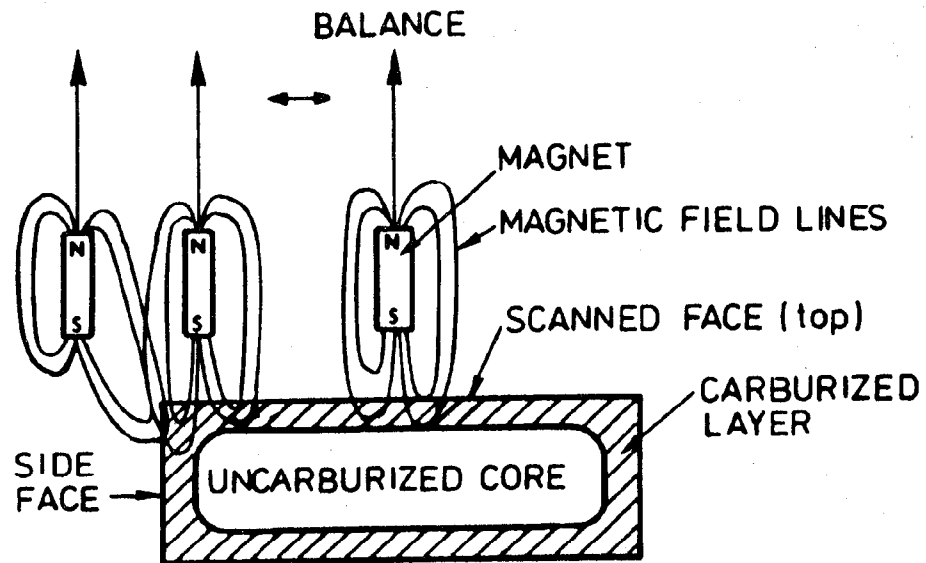
Fig. 11   Schematic presentation of the magnetic response of a carburized specimen at
different location of the magnet.
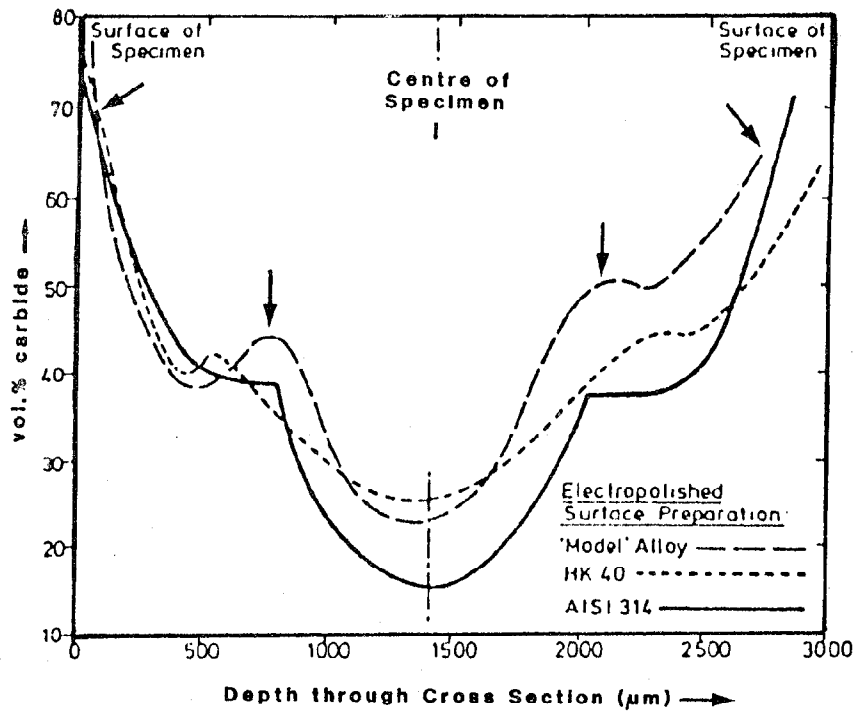
a) different 25/20 CrNi-steels carburised for 100h at 1000°C/0.8a_c.
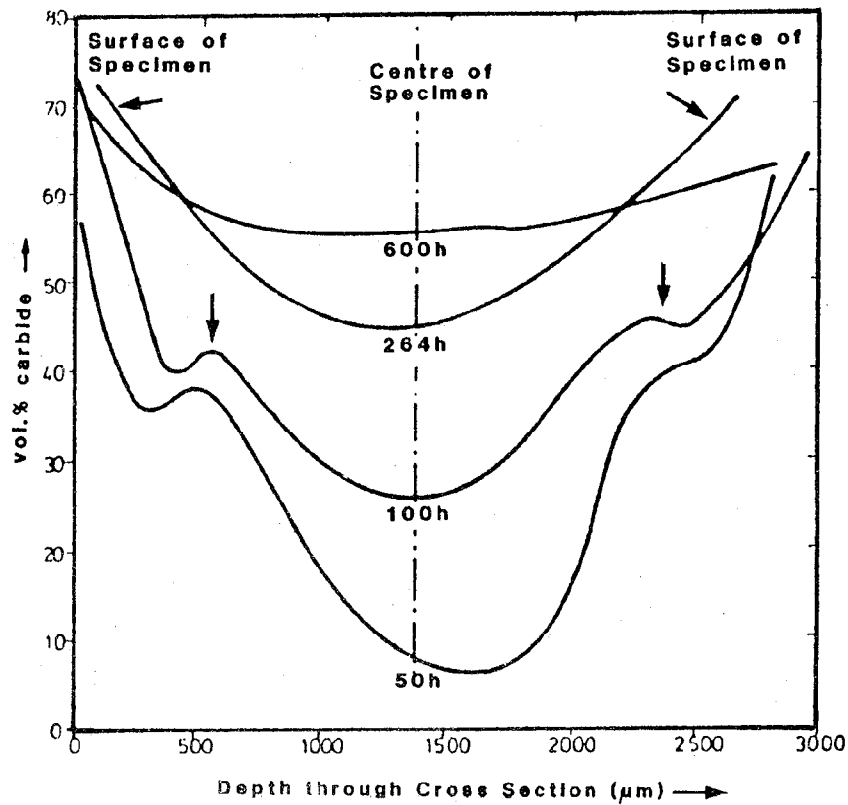
b) HK40 after different exposures at 1000°C/0.8a_c.

Fig. 12: Examples of irregulaties in the carbide (vol%) distribution (indicated by arrows) over the cross-section of various carburised specimens.
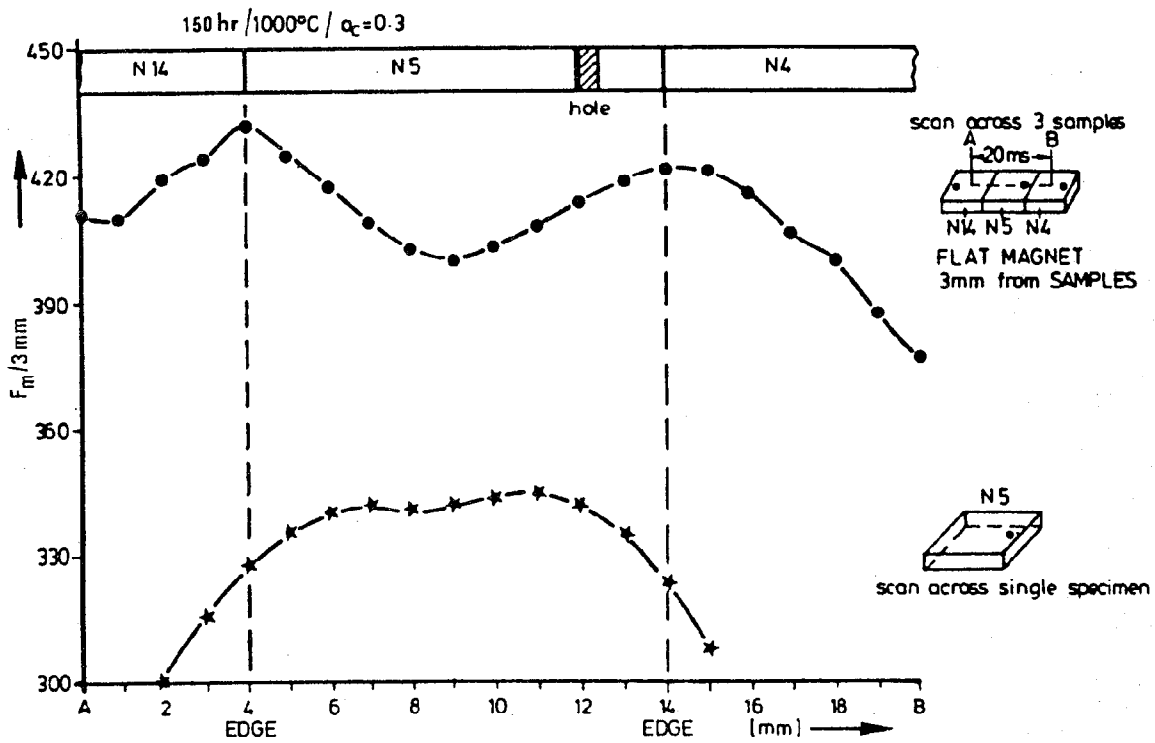
Fig. 13   "Edge effect" when scanning a single specimen,
and the same specimen surrounded by two similar ones.
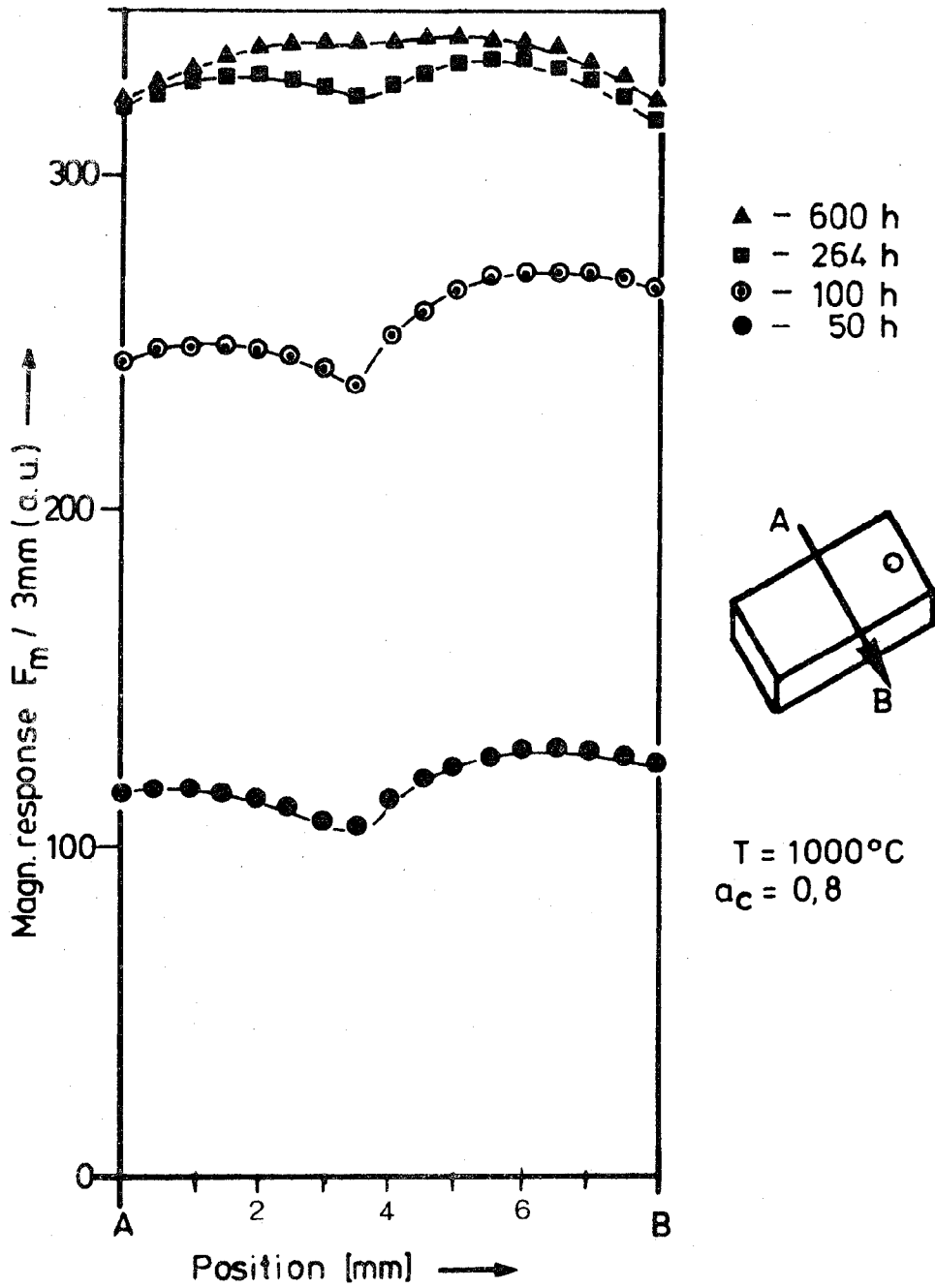
Fig. 14   Magnetic response scan of an AISI 314 specimen after different periods of
carburization at 1000 °C (a_c = 0.8).
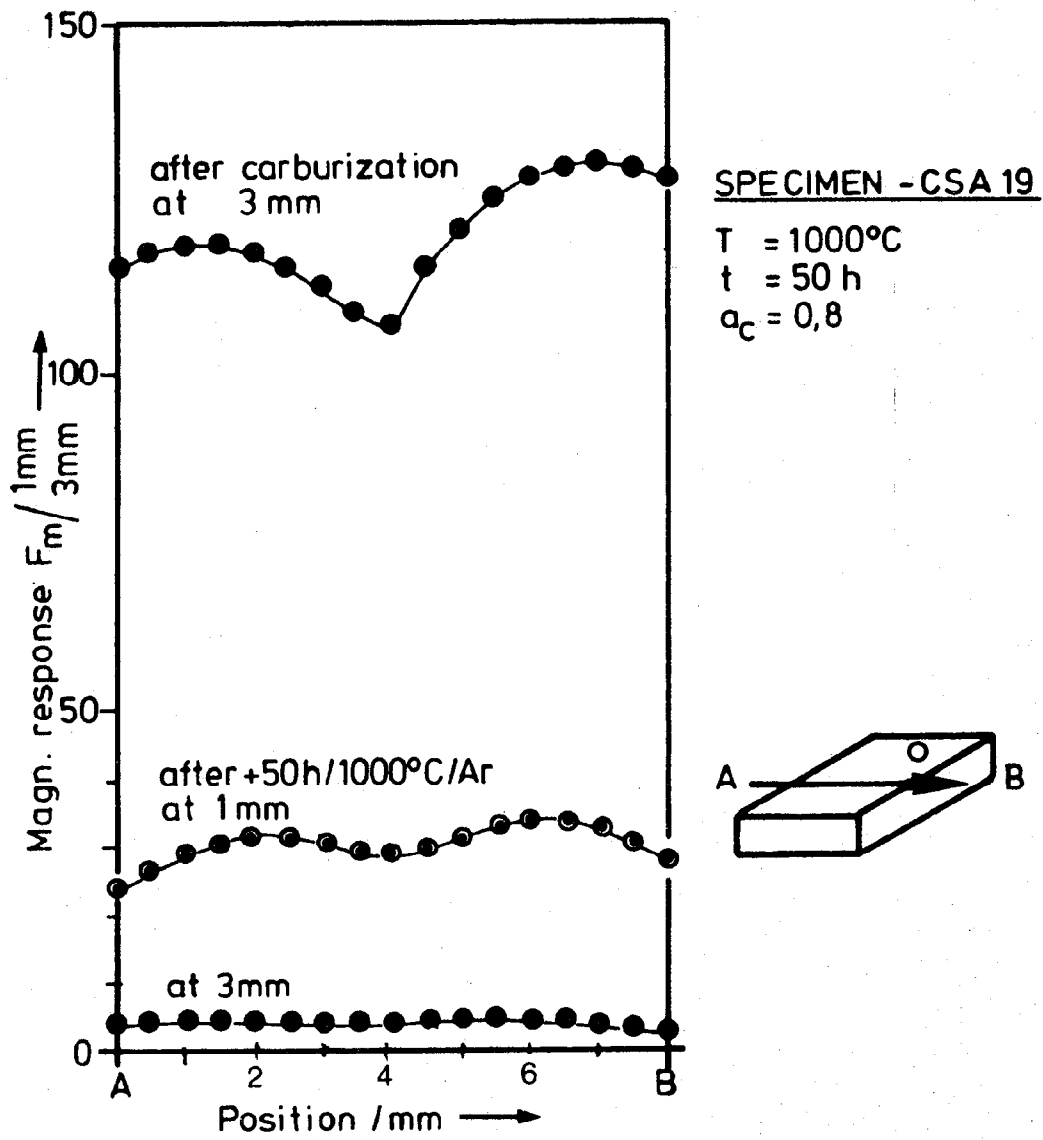
Fig. 15a Alteration of the magnetic response of a carburized specimen by annealing for 50 hr at 1000 °C in Argon.

M_7C_3

$M_{23}C_6$

Pepperhoff
125x

M_7C_3

$M_{23}C_6$

Murakami's
63x

i)   ii)
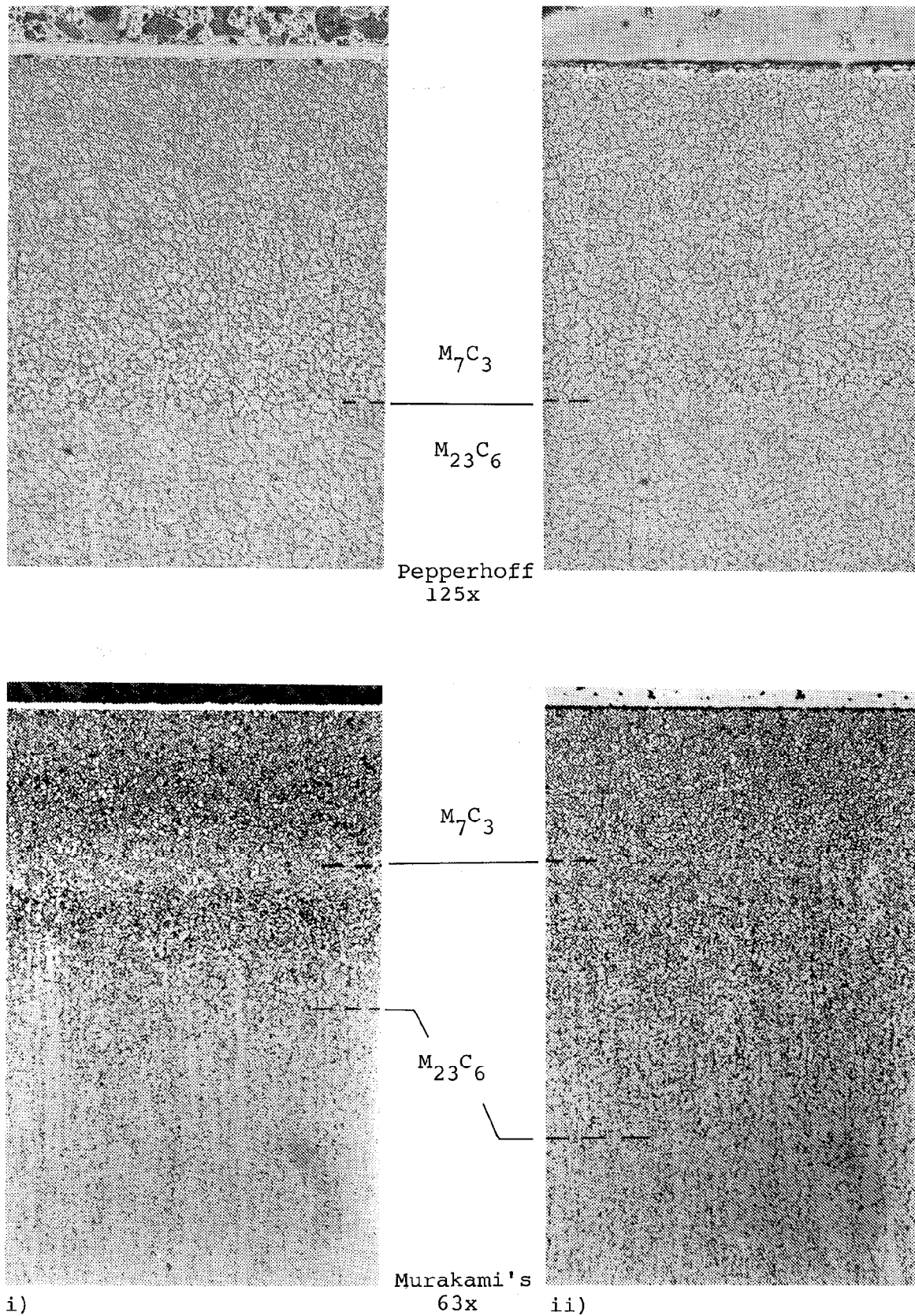
Fig. 15b   Microstructure of AISI 314 specimen
i)   after exposure to 0.8 a_c environment at 1000 °C for 50 hrs,
ii)   after subsequent ageing in Argon at 1000 °C for 50 hrs.
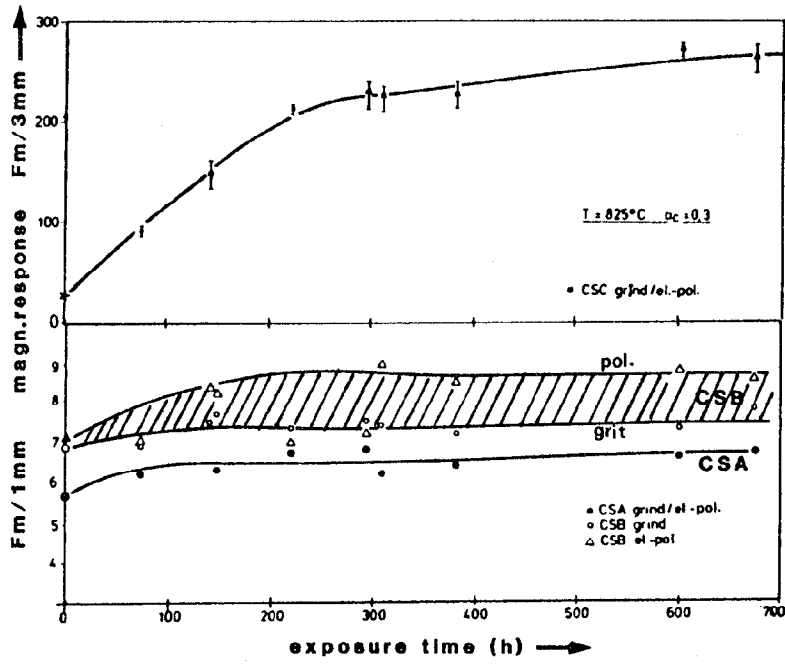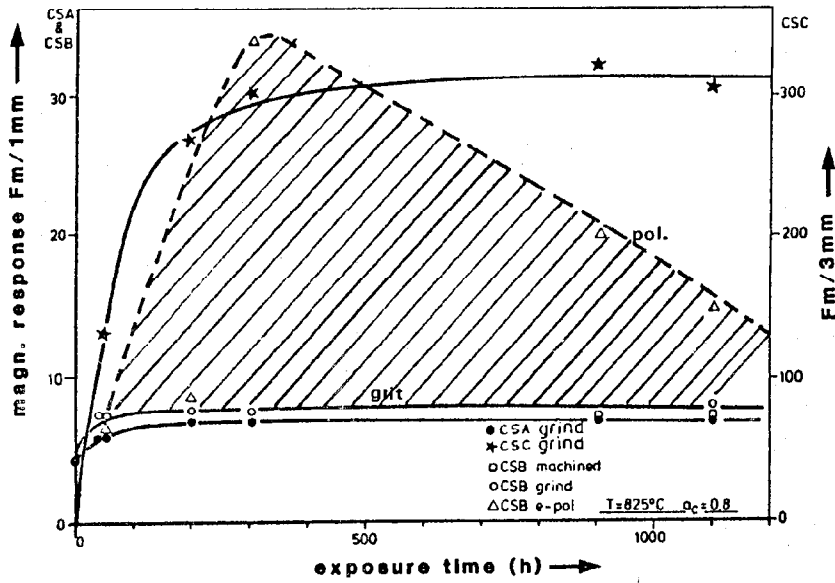
Fig. 16   Variation of magnetic response of 25/20CrNi alloys as a function of
carburization time at 825 °C, for different carbon activities

a) $a_c = 0.3$;   b) $a_c = 0.8$
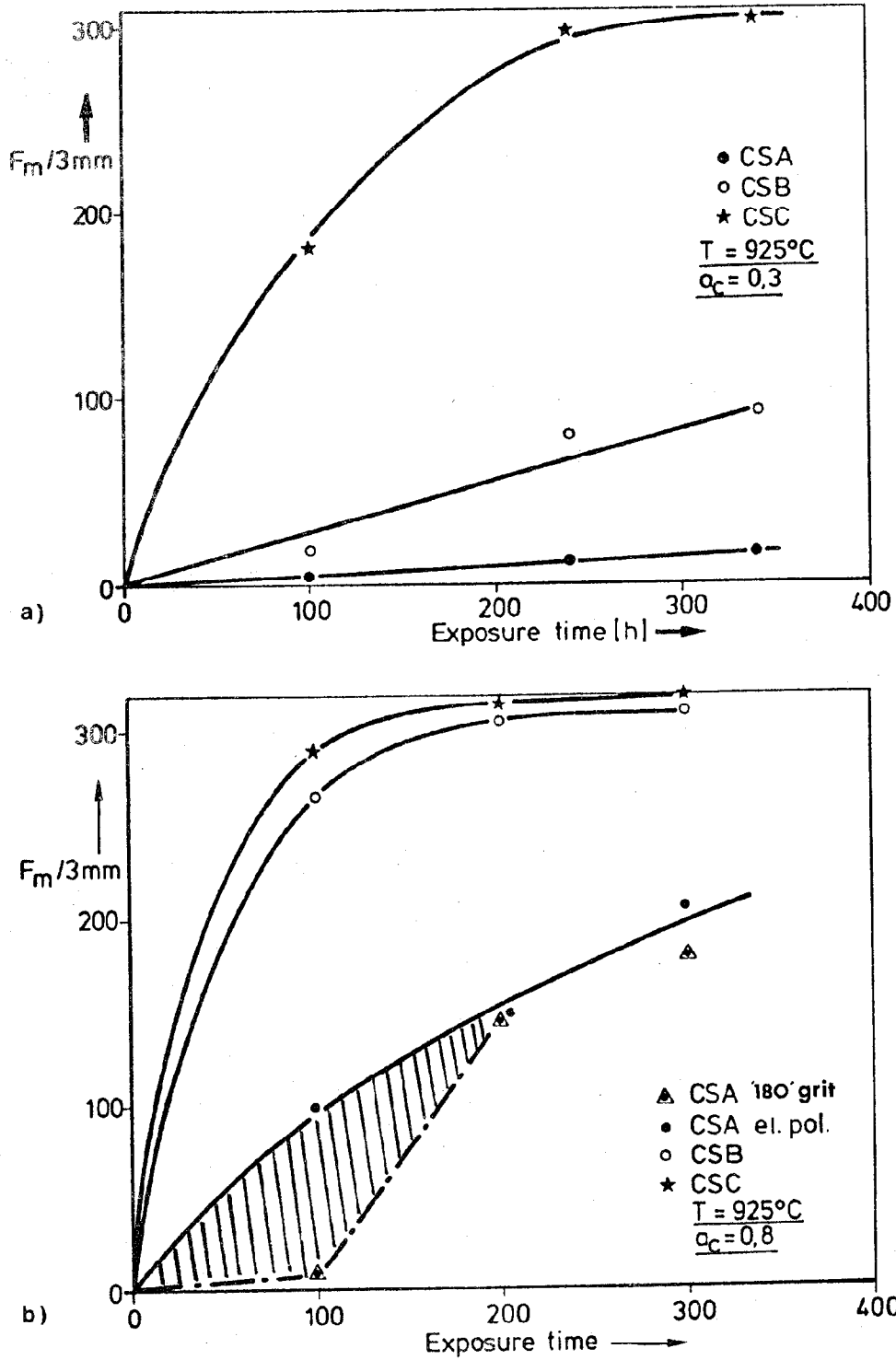
Fig. 17   Variation of magnetic response of 25/20Cr/Ni alloys as a function of carburization
time at 925 °C
a)   0.3 a_c ;   b)   0.8 a_c .
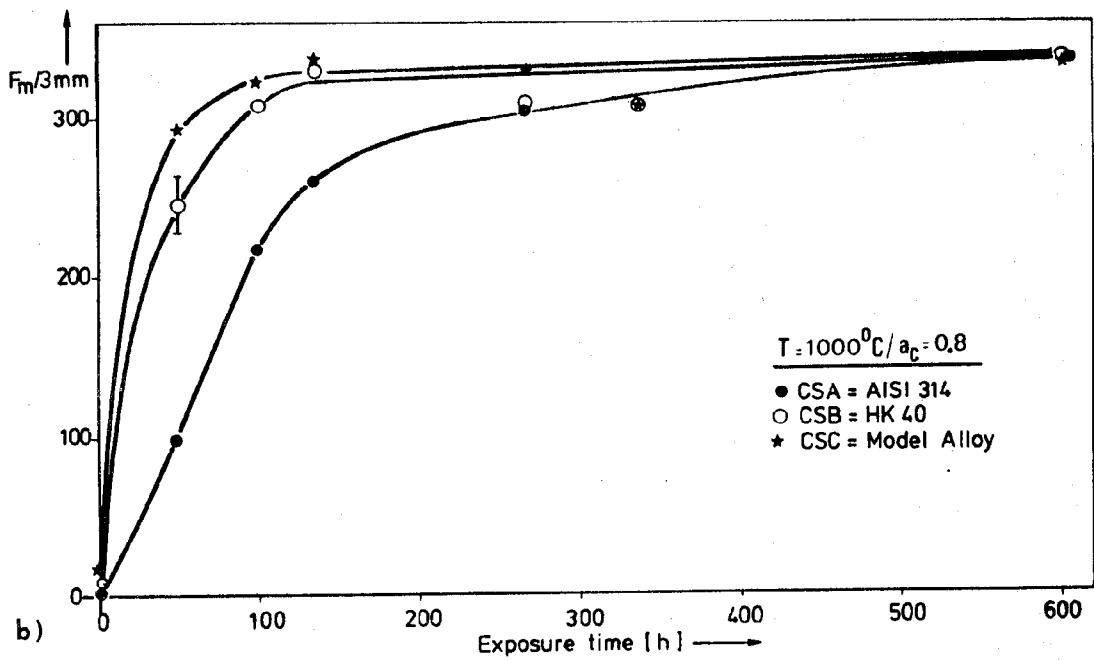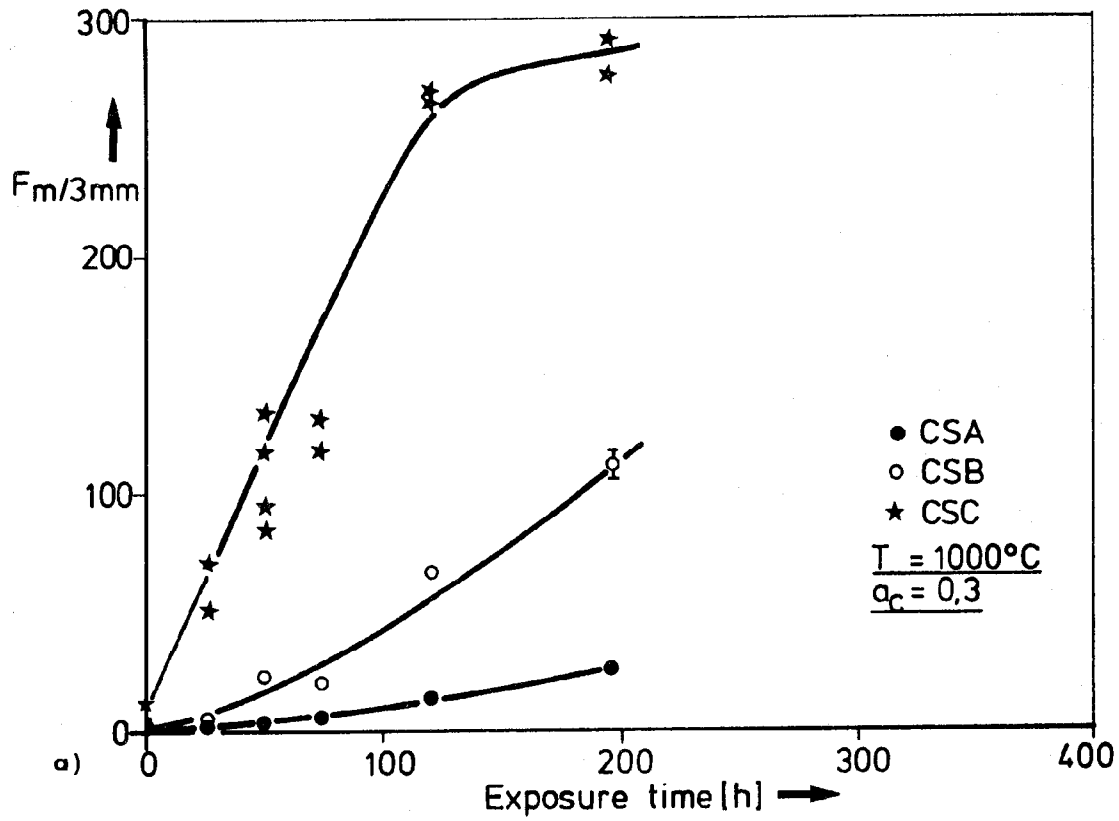
Fig. 18   Variation of magnetic response of 25/20 CrNi steels as a function of
carburization time at 1000 °C and 0.3 a_c (a) and 0.8 a_c (b) respectively.
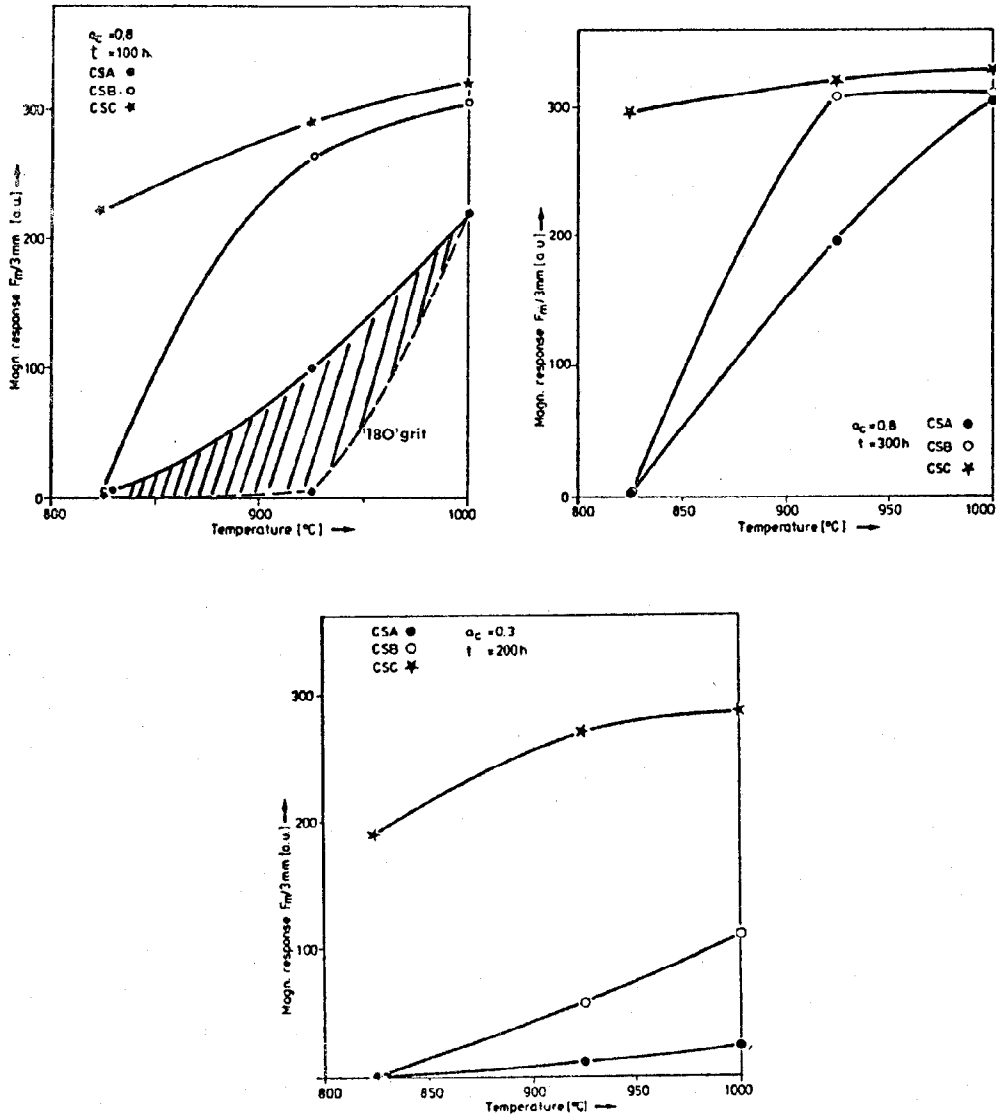
Fig. 19   Change in magnetic response at various temperatures for the exposure conditions
indicated. (materials electropolished except where indicated differently).

Fig. 20   Correlation of weight change data with magnetic response.
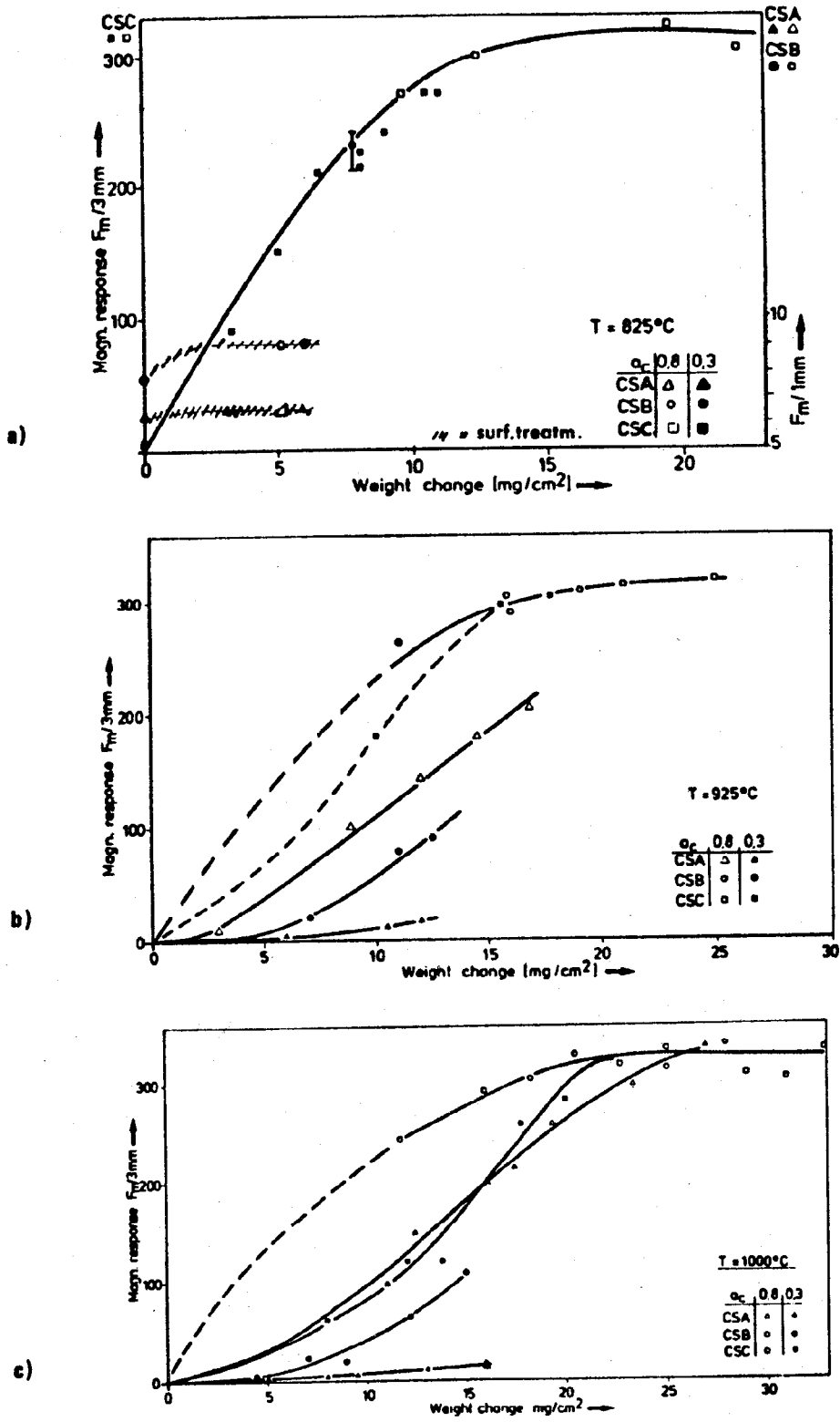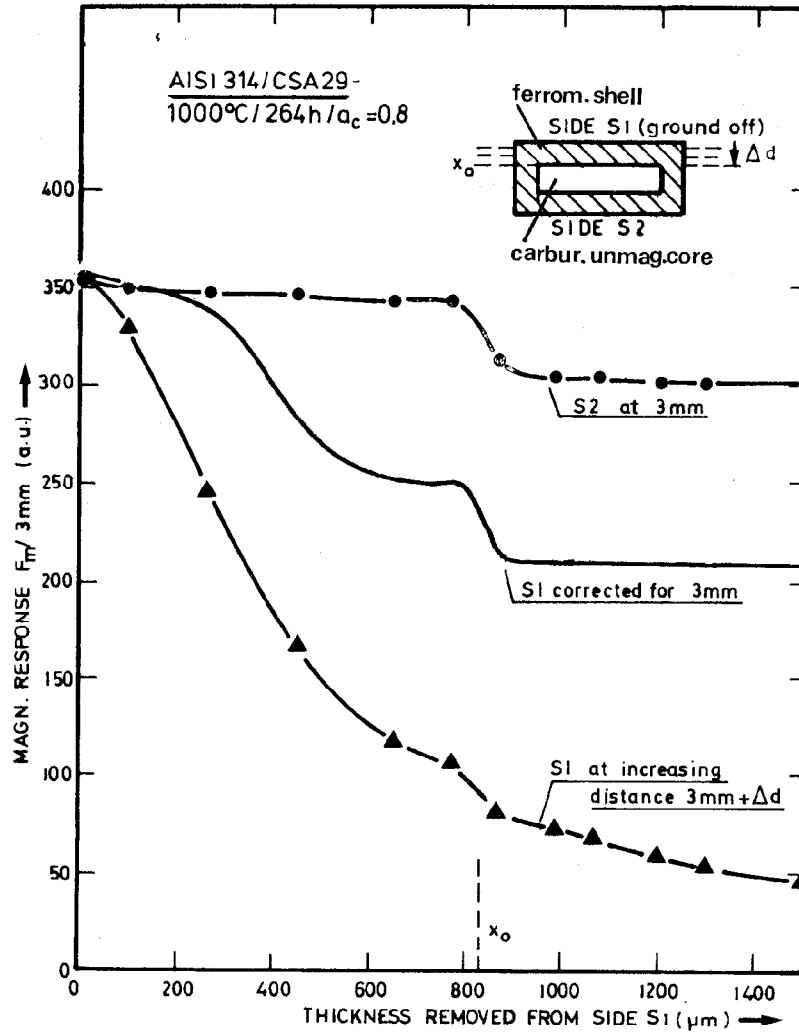
a)
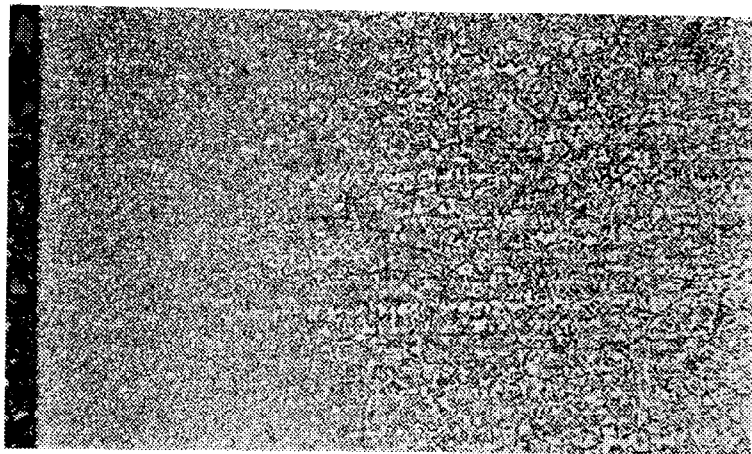
b)   x 63

Fig. 21   a)   Variation of magnetic response through a carburized specimen
           b)   Optical microsection of the specimen.
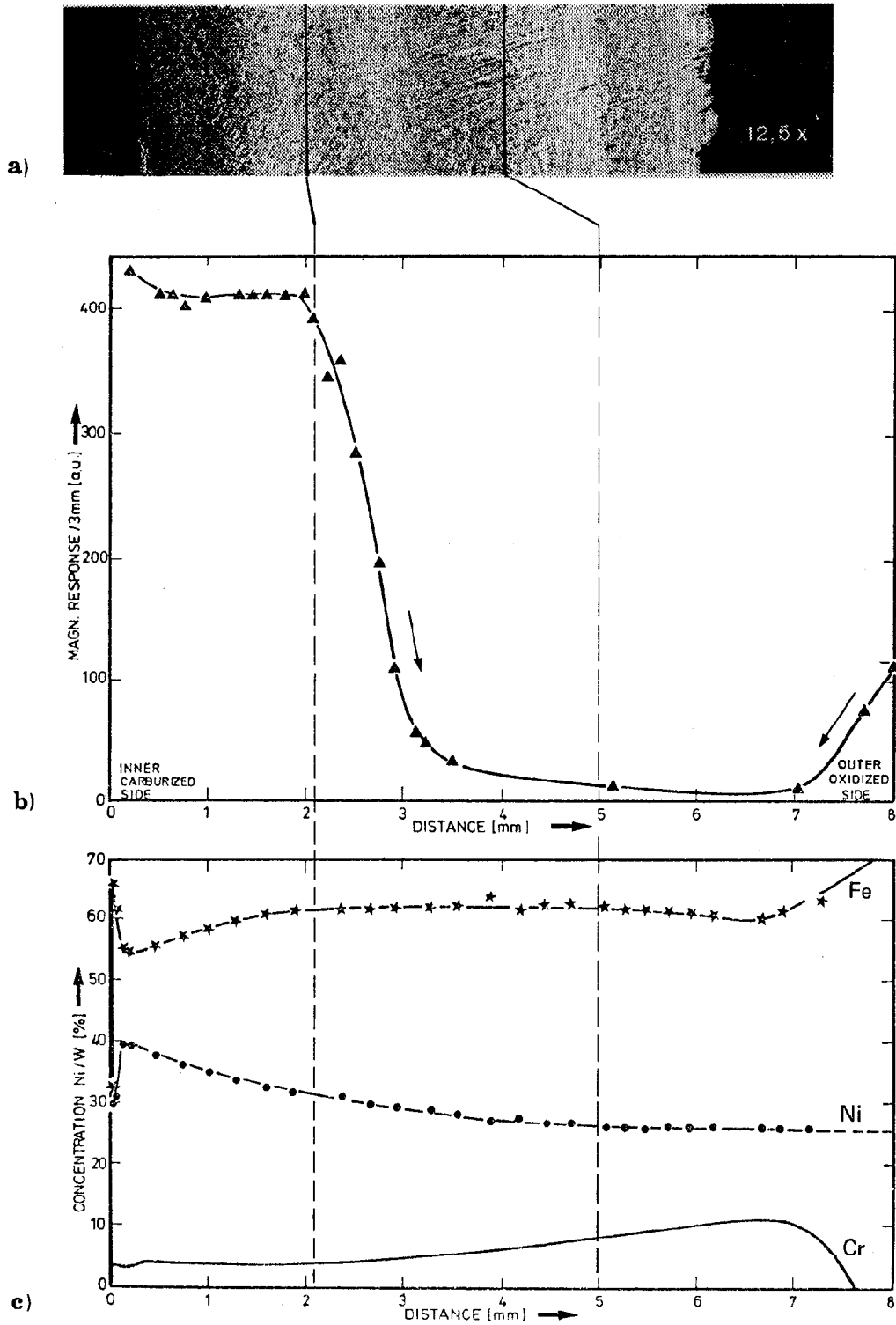
Fig. 22   a)   Microstructure of carburized HK40 tube section.
          b)   Variation of F_m with removal of material from the inner tube **surface**
          c)   Composition profiles of Fe, Ni, Cr of the austenitic matrix cross-section.
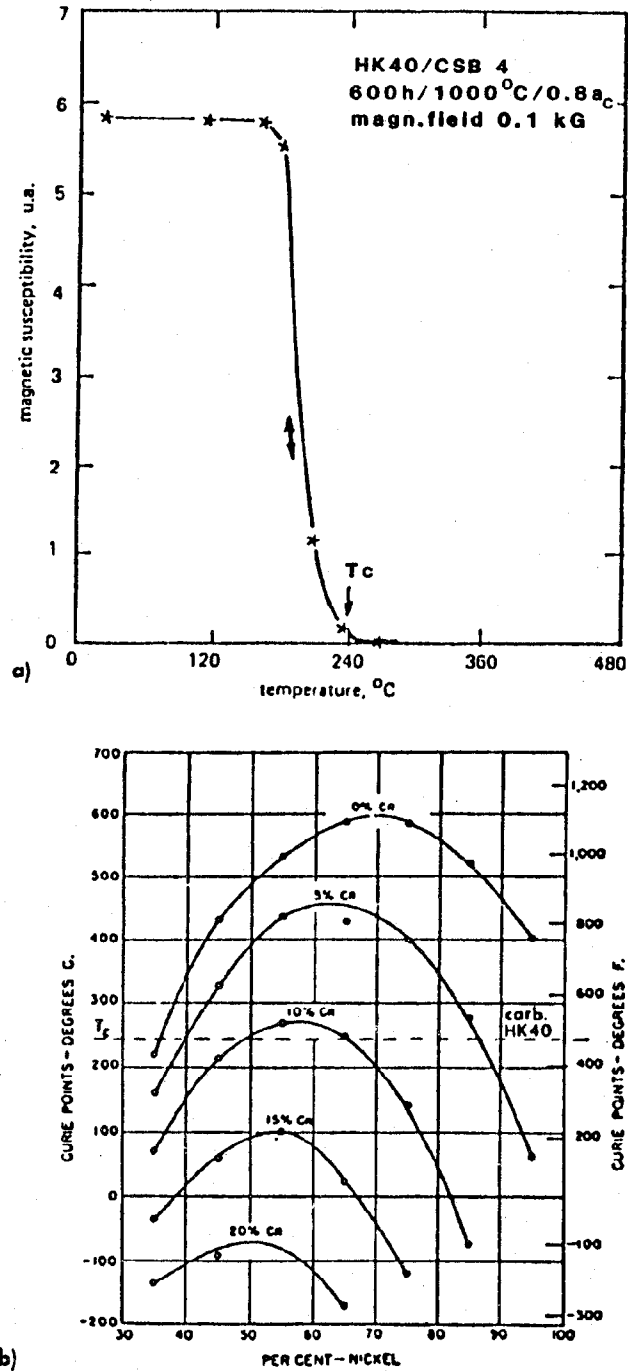
Fig. 23 a) Variation of magnetic susceptibility with temperature of a carburized HK40
              specimen (1000 °C/ 0.8 a_c).
         b) Variation of Curie-temperature of FeNiCrSi-alloys with Cr-content (after
              Jackson and Russel (13)).
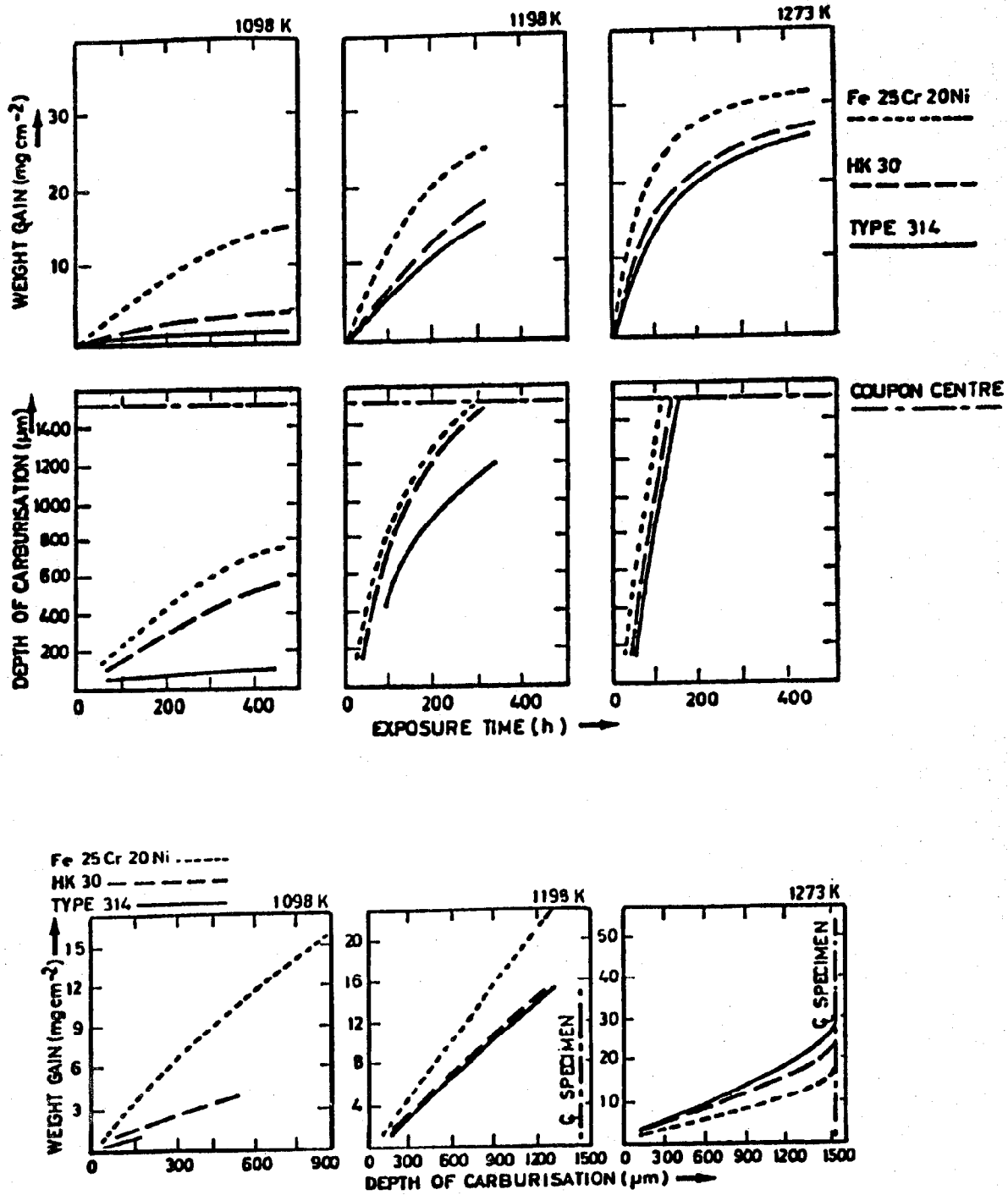
Fig. 24: Correlation between gravimetric and metallographic estimation of carburisation at 1098, and 1273 K in 0.8 carbon activity gas, electropolished surface finished. (after 19)

Appendix I

Effect of various experimental parameters on magnetic response
measurements

The measurements of the magnetic response of carburised samples by the
Rankine-balance-system are dependent upon a number of experimental
parameters, as briefly outlined already in § 3.

First of all it is obvious from the fundamental equation :

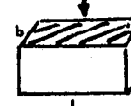$$F_m = m \cdot \chi \cdot H \, \delta H / \delta x \qquad (1)$$
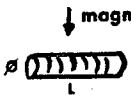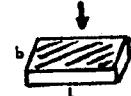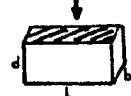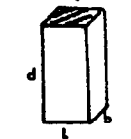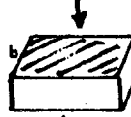
that the magnetic force is proportional to the field strength and
gradient of the magnet. Therefore throughout this study, the same magnet
was used, the field strength of which was frequently checked for
constancy.

Since the strength (H) and the gradient ($\delta H / \delta x$) of the magnetic field
decrease significantly with distance, the magnetic response obviously
depends on the distance between magnet and sample as shown in fig. 1.1.
Because of the much higher sensitivity at small distances, a measuring
distance of 1 mm was used for materials with low magnetic response, while
in most other cases the measurements were taken at 3 mm. Only
measurements taken at the same distance are directly comparable, although
readings taken at different distances might be converted by using a
calibration curve for the material under investigation, as shown in
fig. 1.1.

According to equation (1), the magnetic responsed measured with a magnet
at a constant distance on a material of susceptibility, χ, should be
proportional the mass, m, of the sample.

However, measurements on Nickel-samples of constant mass but different
shape, i.e. different thickness and surface area exposed to the magnet,
indicated (table I) that apparently not only the mass of a specimen
determines its magnetic response, but also its shape, i.e. surface and/or
thickness.

Table I : F_m-readings of Ni-pieces with equal mass but different shape.

Specimen shape		Mass	exposed area	$F_m/3$ mm (a.u.)
↓ magnet ø (cylinder)	ø= 5mm L=11mm	1.864 g	0.216 cm^2	250
↓ (slab)	L=15 mm b= 6 mm d= 3 mm	1.864 g	0.90 cm^2	324
↓ (slab)	L=15 mm b= 3 mm d= 6 mm	1.864 g	0.45 cm^2	257
↓ (block)	L= 3 mm b= 6 mm d=15 mm	1.864 g	0.18 cm^2	147
↓ (slab)	L=6.5 mm b=5 mm d=1 mm	0.1948 g	0.33 cm^2	131
↓ (slab)	L=6.5 mm b=1 mm d=5 mm	0.1948 g	0.07 cm^2	97

Measurements on Ni-samples of constant surface area (0.8 cm^2) but varying thickness are shown in Fig. 1.2 and reveal that the F_m-signal (measured at a constant distance of 3 mm between magnet and sample surface) is increasing continuously – in a non-linear fashion – to about 0.5 mm only. For still thicker specimens the measured magnetic response essentially remains constant.

It is interesting to mention here that measurements on a piece of NIMONI 75, a Ni-Cr alloy with much lower susceptibility, showed a rather similar behaviour at a much lower level of F_m (i.e. measurements at 1 mm distance).

A similar behaviour was observed when measuring specimens of constant thickness (2 mm) but varying surface area, as shown in Fig. 1.3 : First the magnetic response increases steeply with increasing surface, but then the rate slows down and for sample surfaces > 4 cm^2 achieves constant values. Hence for surfaces smaller than 4 cm^2 measurements taken with the present magnet will depend strongly on the surface area exposed to the magnet.

The features described above which can be described as "limited reach" of the magnet used can be explained by the fact that the fundamental boundary condition of equ.(1), i.e. all volume elements of the assessed specimen should be exposed to the same field parameter (H.δH/δx) is not fulfilled since :

i)   the volume of our samples is not infinitely small, and

ii)   as showed above, the magnetic field strength (H) and gradient
      (δH/δx) are varying strongly with distance from the magnet.

Some of the critical factors determining the value of the F_m-signal have been eliminated in the present study by

i)   using the same magnet throughout the investigations,
ii)   keeping the distance between the magnet and sample constant (3 mm),
iii) comparing samples of equal shape and surface area.

Considering the above results, there remain, however, some doubts as to what extent the foregoing measurements on carburised specimens have been influenced by the generally observed limited relationship between the mass of magnetic material and the recorded F_m-signal.
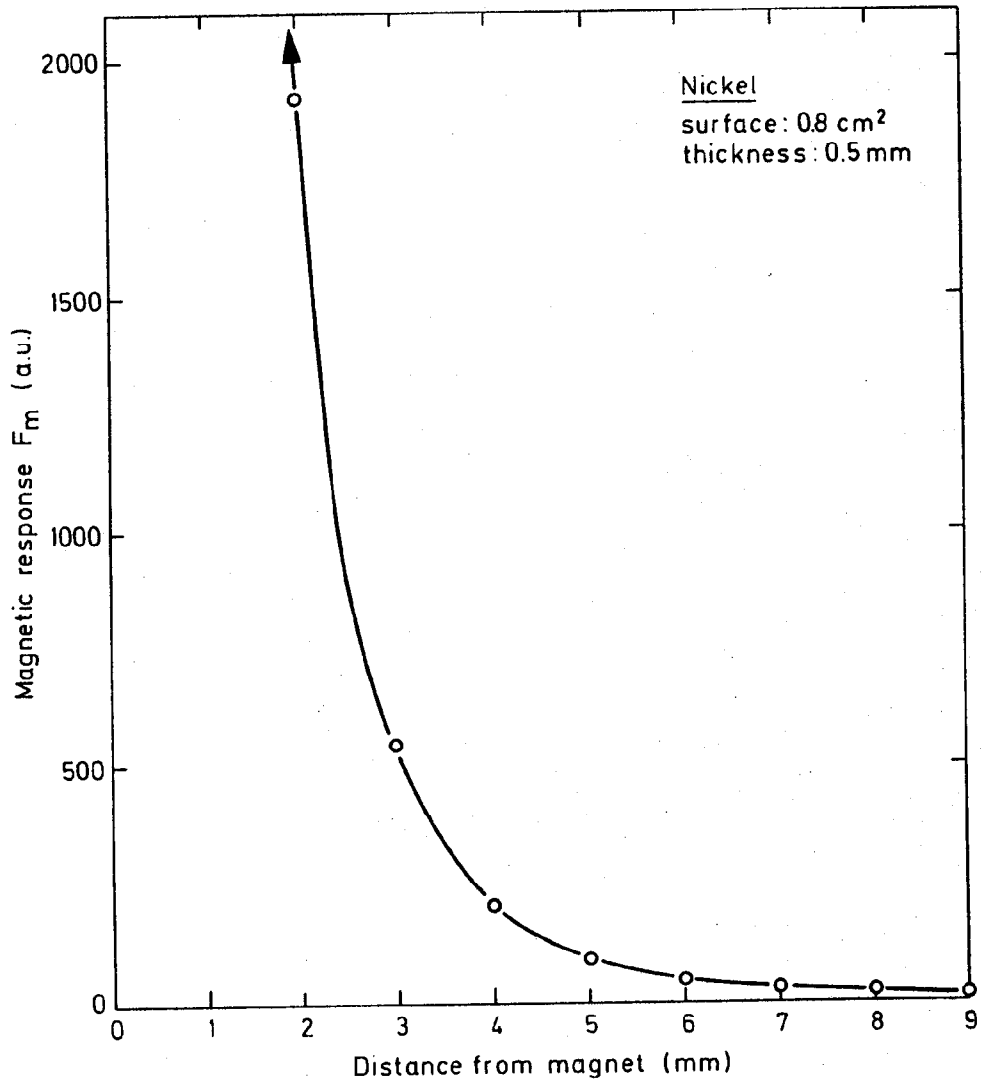
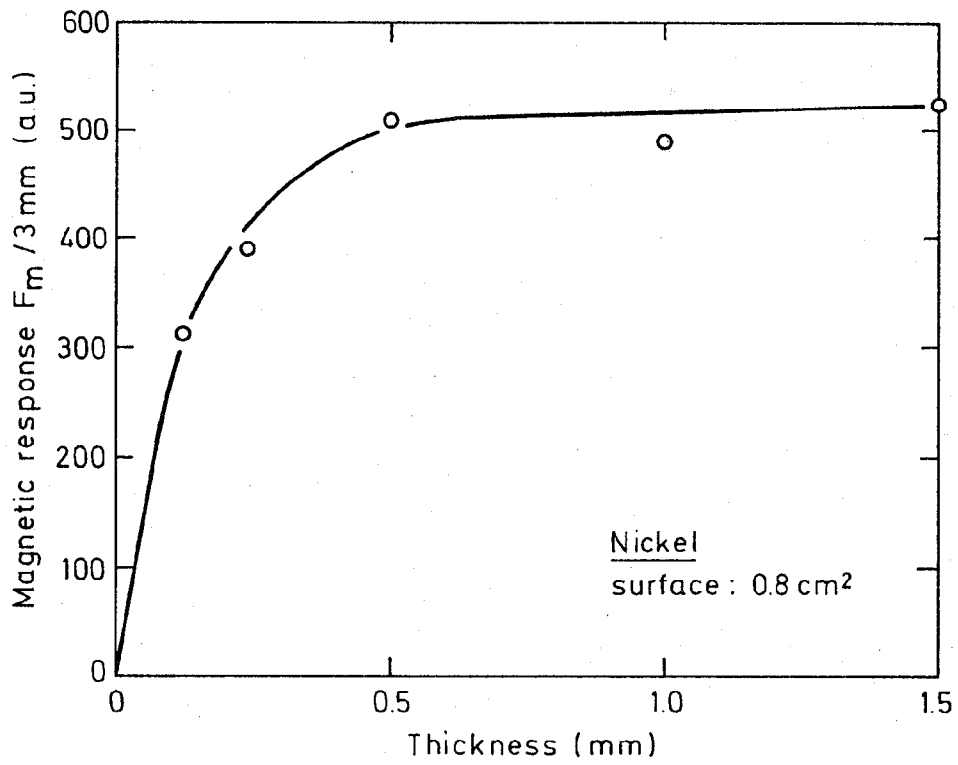Fig. 1.1: Variation of magnetic response as function of distance magnet/sample.

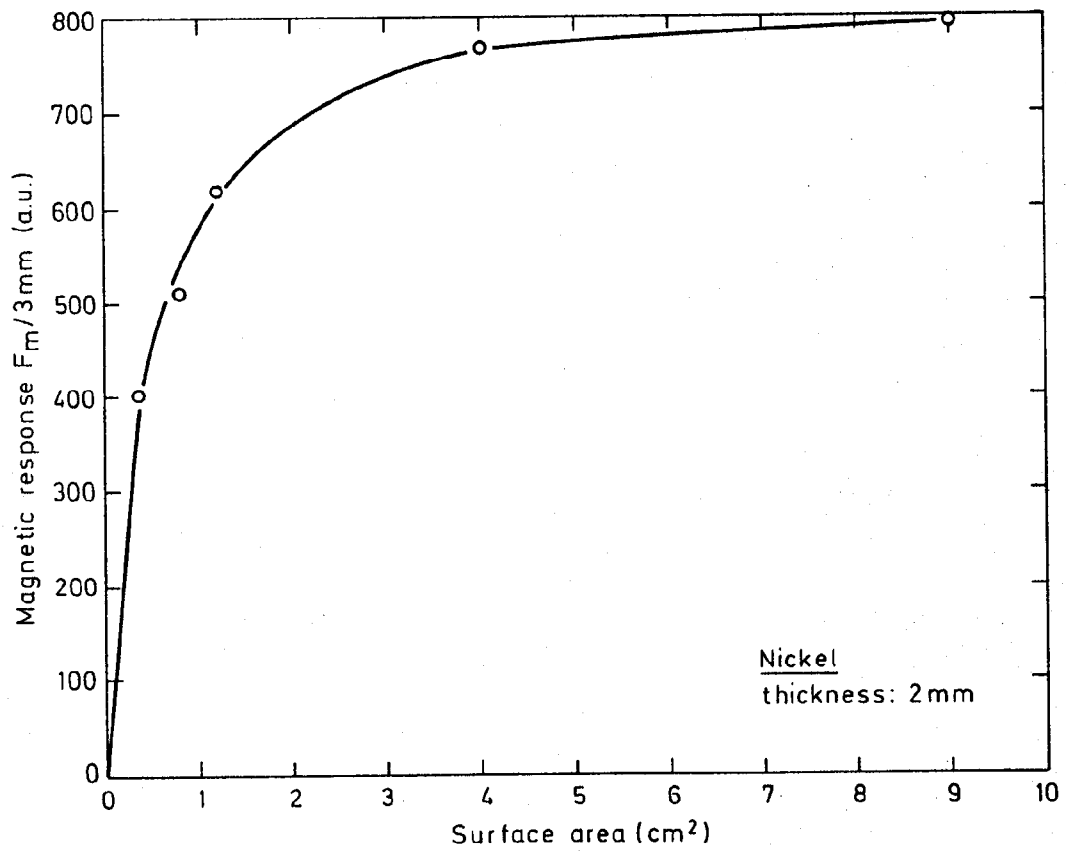Fig. 1.2: Variation of magnetic response as function of sample thickness.

Fig. 1.3: Variation of magnetic response as function of sample surface area.